

Mesoscopic fluctuations of the supercurrent in diffusive Josephson junctions

Manuel Houzet¹ and Mikhail A. Skvortsov²

¹*Commissariat à l'Énergie Atomique, DSM/DRFMC/SPSMS, 38054 Grenoble, France*

²*Landau Institute for Theoretical Physics, Chernogolovka, Moscow region, 142432 Russia*

(Dated: April 25, 2007)

We study mesoscopic fluctuations and weak localization correction to the supercurrent in Josephson junctions with coherent diffusive electron dynamics in the normal part. Two kinds of junctions are considered: a chaotic dot coupled to superconductors by tunnel barriers and a diffusive junction with transparent normal–superconducting interfaces. The amplitude of current fluctuations and the weak localization correction to the average current are calculated as functions of the ratio between the superconducting gap and the electron dwell energy, temperature, and superconducting phase difference across the junction. Technically, fluctuations on top of the spatially inhomogeneous proximity effect in the normal region are described by the replicated version of the σ -model. For the case of diffusive junctions with transparent interfaces, the magnitude of mesoscopic fluctuations of the critical current appears to be nearly 3 times larger than the prediction of the previous theory which did not take the proximity effect into account.

PACS numbers: 74.40.+k, 74.45.+c, 74.50.+r, 73.20.Fz

I. INTRODUCTION

At low temperatures, conductance of metals is due to electron scattering on impurities. The wave nature of electron motion reveals in a number of quantum interference effects: the weak localization (WL) correction¹ to the classical Drude conductance, and universal sample-to-sample conductance fluctuations.^{2,3} In mesoscopic samples whose size does not exceed the phase coherence length, $L_\phi(T)$, the magnitude of conductance fluctuations characterized by the root mean square (rms) δG is independent on the system size and degree of disorder and is of the order of the conductance quantum $G_Q = e^2/\pi\hbar$. Weak localization corrections and universal conductance fluctuations have attracted considerable interest since the 80s' both from the experimental and theoretical sides.⁴

Two years after discovery of conductance fluctuations in metals, Altshuler and Spivak⁵ applied the same idea to fluctuations of the supercurrent in Josephson junctions formed of a diffusive normal metal (N) placed between two superconducting (S) leads. They considered the limit of *long* junctions, when the Thouless energy $E_T = \hbar D/L^2$ (D is the diffusion constant and L is the length of the junction) is much smaller than the superconducting gap Δ in the leads. In particular, it was found in Ref. 5, that for quasi-one-dimensional long wires, mesoscopic fluctuations of the critical current are characterized by the rms $\delta I_c = \sqrt{3\zeta(3)} eE_T/\pi\hbar = 0.60eE_T/\hbar$ at zero temperature.

The theory of Ref. 5 was based on the standard diagrammatic technique operating with soft diffusive modes – diffusons and Cooperons – but Andreev reflection at the NS interface⁶ was described by the *linear* phenomenological boundary conditions on diffusive modes⁷. However, the proximity effect in SNS systems is known to be essentially nonperturbative at low energies, where Cooper pairs penetrating from a superconductor strongly mod-

ify electronic properties and open a minigap E_* in the normal region.⁸ This strong perturbation of the metallic state can be described only with the help of the full set of *nonlinear* Usadel equations⁹ (in diffusive systems). Thus, the treatment of Ref. 5, which effectively considered mesoscopic fluctuations of the supercurrent on top of a uniform metallic state without a minigap, is not accurate and should be reconsidered taking the proximity effect into account nonperturbatively.¹⁰

Extensive studies of the proximity effect in SNS systems^{11–14} demonstrate that the critical Josephson current is related to the minigap induced in the normal region: $I_c \sim GE_*/e$, where G is the normal-state conductance of the junction. On the other hand, the minigap can be roughly estimated as $E_* \sim \min(\Delta, E_{\text{dwell}})$, where Δ is the superconducting gap, and $E_{\text{dwell}} = \hbar/t_{\text{dwell}}$ is the energy associated with the typical dwell time t_{dwell} of an electron in the normal region. Since mesoscopic fluctuations for quantum dots and quasi-one-dimensional systems are usually small in the parameter G_Q/G , one can estimate the magnitude of mesoscopic fluctuations as $\delta I_c \sim eE_*/\hbar$. For a long diffusive wire, $E_{\text{dwell}} \sim E_T$, indicating that results of Ref. 5 are qualitatively correct.

The scattering matrix approach¹⁵ has proven to be a powerful tool for studying coherent electron transport in mesoscopic conductors. In the framework of this approach, an arbitrary scatterer can be described by a set of transparencies in each conduction channel. The main transport characteristics of a mesoscopic conductor, such as the conductance, shot noise power, conductance of the NS junction, can be written as a linear statistics on the transmission eigenvalues, $\sum_n f(T_n)$.¹⁵ Then, the corresponding weak localization corrections and mesoscopic fluctuations can be determined from the knowledge of the average density and the correlation function of transmission eigenvalues. For a diffusive wire, they were obtained in Refs. 16,17. However, the Josephson current is generally *not* a linear statistics on T_n 's. It

is a linear statistics only for a *short* ($\Delta \ll E_T$) wire:¹⁸ $I(\chi) = (e\Delta/2\hbar) \sum_n T_n \sin \chi / [1 - T_n \sin^2(\chi/2)]^{1/2}$, where χ is the superconducting phase difference. In this limit one finds for the fluctuations of the critical current at zero temperature:^{16,17} $\delta I_c \simeq 0.30(e\Delta/\hbar)$. The crossover between short and long wires was also considered numerically within the tight-binding model.¹⁹

Recently, the problem of mesoscopic fluctuations of the supercurrent in short junctions with weakly transparent NS interfaces was considered by Micklitz²⁰ who used the machinery of the supersymmetric nonlinear σ -model²¹. Within that approach, the average Josephson current is obtained at the level of the saddle point which corresponds to the quasiclassical Usadel equations²², while mesoscopic fluctuations can be obtained from fluctuations around the saddle point. We believe that the functional σ -model approach is a proper tool for studying mesoscopic fluctuations of the Josephson current, especially in the limit of long junctions where the multiple scattering theory fails.

A couple of experiments with the use of a gated semiconductor instead of a normal metallic part have been reported.^{23,24} Mesoscopic fluctuations were observed with varying the gate voltage. In Ref. 23, mesoscopic fluctuations were shown to follow precisely those of G , the latter being estimated from $I(V)$ curves at a bias voltage larger than the superconducting gap. On the other hand, δI_c was systematically found to be smaller than the theoretical estimate from Ref. 5. A similar behavior was reported in Ref. 24.

In this work, we present the derivation of mesoscopic fluctuations, $\delta I(\chi) = [\langle I^2(\chi) \rangle - \langle I(\chi) \rangle^2]^{1/2}$, and weak localization correction, $\Delta_{\text{WL}} I(\chi)$, to the Josephson current in diffusive SNS junctions within the replicated version of the nonlinear σ -model. We ignore interaction effects in the normal metal and assume zero magnetic field. By expanding the action of the σ -model around its saddle point, corresponding to an inhomogeneous solution of the Usadel equations, we present mesoscopic fluctuations in terms of the soft modes, analogous to Cooperons and diffusons in the normal state^{20,22}. This approach allows us to follow the crossover between the regimes of short and long wires.

In general, we verify that for the Josephson current through a chaotic dot and quasi-one-dimensional wire, $\delta I_c/I_c \sim -\Delta_{\text{WL}} I_c/I_c \sim G_Q/G$, where G is the normal-state conductance of the system, and determine the exact coefficients in these relations as functions of the junction length and temperature. These coefficients are generally of the order of 1, but in some cases (two tunnel barrier structures with low barrier transparency) are additionally suppressed.

In particular, we find that the approach of Ref. 5 which does not take the proximity effect into account systematically underestimates rms I_c by the factor of order 3. In the limit of long ($E_T \ll \Delta$) quasi-one-dimensional junc-

tions at zero temperature, we obtain

$$\delta I_c = 1.49 \frac{eE_T}{\hbar}, \quad (1)$$

which is 2.5 times larger than the prediction of Ref. 5. Similarly, for wide ($W_x, W_y \gg L$) and long ($E_T \ll \Delta$) three-dimensional junctions made of a metallic parallelepiped of size $L \times W_y \times W_z$, we find at $T = 0$:

$$\delta I_c = 2.0 \frac{eE_T}{\hbar} \sqrt{\frac{W_y W_z}{L^2}}, \quad (2)$$

which is 2.8 times larger than the corresponding result of Ref. 5.

The paper is organized as follows. In Section II, we consider the case of a chaotic diffusive dot coupled to the superconducting leads through tunnel barriers. This model allows us to introduce the method and is simple enough to be solved analytically. In Section III, we consider the case of a diffusive wire with transparent NS interfaces. Mesoscopic fluctuations of the critical current in two-dimensional (2D) and three-dimensional (3D) geometries are calculated in Sec. IV. We discuss the results in Conclusion. Technical details are delegated to several Appendices.

II. SUPERCONDUCTOR-CHAOTIC DOT-SUPERCONDUCTOR JUNCTIONS

As a warm-up, in this section we consider a Josephson junction formed of a “zero-dimensional” chaotic dot in contact with two superconducting reservoirs through tunnel junctions with conductances G_L and G_R . A possible realization of this system would be a short diffusive wire, with the Thouless energy E_T much exceeding the superconducting gap Δ in the superconductors and with the intra-dot conductance $G_N = 2\pi G_Q E_T/\delta$ (where δ is the mean level spacing in the dot) much exceeding G_L and G_R . As a consequence, the conductance of the structure in its normal state is determined solely by the tunnel barriers: $G = G_L G_R / (G_L + G_R)$.

The average Josephson current in such a system has been studied by Aslamazov, Larkin, and Ovchinnikov²⁵ within the tunnel Hamiltonian approach, by Kupriyanov and Lukichev²⁶ with the help of the quasiclassical Usadel equations, and by Brouwer and Beenakker²⁷ using the scattering approach¹⁸ and Random Matrix Theory (RMT)¹⁵. It was found that the amplitude of the supercurrent is controlled by the ratio between the superconducting gap Δ and the “escape” energy $E_g \sim G\delta/G_Q$. The later energy scale is associated to the broadening of levels in the dot due to coupling with the leads, playing here the role of the dwell energy E_{dwell} defined in Introduction.

We shall rederive these results in the fermionic replica σ -model language and then use this formalism to study mesoscopic fluctuations of the Josephson current for arbitrary ratio Δ/E_g . A similar approach was very recently

followed by Micklitz²⁰ who considered the effect of barrier transparencies on the average supercurrent and its fluctuation in the regime $\Delta \ll E_g$, within the framework of the supersymmetric σ -model.

In Sec. II A, we introduce the replica σ -model for this system. In Sec. II B, we analyze its saddle point solution and rederive the quasiclassical result for the Josephson current. The fluctuation determinant is calculated in Sec. II C. It contains both weak localization corrections to the supercurrent and its mesoscopic fluctuations, which are analyzed in Secs. II D and II E. The results are summarized in Sec. II F.

A. Replica σ -model for a chaotic dot

The equilibrium supercurrent which flows in a Josephson junction can be obtained from the free energy $\mathcal{F} = -kT \ln Z$ of the system at temperature T :

$$I(\chi) = \frac{2e}{\hbar} \frac{d}{d\chi} \mathcal{F}(\chi), \quad (3)$$

where χ is the superconducting phase difference between the leads. Disorder-averaging is performed in a standard way using the replica trick,²⁸

$$\langle \mathcal{F}(\chi) \rangle = -kT \lim_{n \rightarrow 0} \frac{\langle Z_\chi^n \rangle - 1}{n}, \quad (4)$$

where $\langle Z_\chi^n \rangle$ can be evaluated as a functional integral within the fermionic replica σ -model:²⁹⁻³¹

$$\langle Z_\chi^n \rangle = \int \mathcal{D}Q e^{-S[Q]}. \quad (5)$$

The nonlinear σ -model is a field theory formulated in terms of the matrix field Q acting in the direct product of the replica space of dimension n , infinite Matsubara energy space, two-dimensional Gorkov-Nambu space (Pauli matrices τ_i), and two-dimensional spin space (Pauli matrices σ_i). The Q matrix is subject to the nonlinear constraint $Q^2 = 1$ and obeys the charge conjugation symmetry:

$$Q = \bar{Q} \equiv \tau_1 \sigma_2 Q^T \sigma_2 \tau_1, \quad (6)$$

where Q^T stands for the full matrix transposition. The condition (6) is related to simultaneous introduction of the Gorkov-Nambu and spin spaces, which renders the vectors $\Psi = (\psi_\uparrow, \psi_\downarrow^*, \psi_\downarrow, -\psi_\uparrow^*)^T$ and Ψ^* be linearly dependent. The functional integration in Q is performed over an appropriate real submanifold of the complex manifold defined by the constraints $Q^2 = 1$ and $Q = \bar{Q}$.

The action of the σ -model for a chaotic dot coupled to the superconducting terminals via tunnel junctions is given by³²

$$S[Q] = -\frac{\pi}{2\delta} \text{tr} \left(\epsilon \tau_3 Q + \sum_{i=L,R} \frac{G_i \delta}{4\pi G_Q} Q_i Q \right). \quad (7)$$

Here, $\delta = (\nu V)^{-1}$ is the mean level spacing in the dot (V is the dot's volume and ν is the single-particle density of states at the Fermi energy per one spin projection), ϵ is the fermionic Matsubara energy, and the trace is taken over all spaces of the Q matrix.

In the superconducting reservoirs with the order parameters $\Delta e^{-i\chi/2}$ (left) and $\Delta e^{i\chi/2}$ (right), the matrices Q_i ($i = L, R$) are unit matrices in the replica and spin spaces, being diagonal in the energy space with the matrix elements:

$$Q_{L,R} = \left(\tau_1 \cos \frac{\chi}{2} \pm \tau_2 \sin \frac{\chi}{2} \right) \sin \theta_s + \tau_3 \cos \theta_s, \quad (8)$$

where $\cos \theta_s = \cos \theta_s(\epsilon) = \epsilon / \sqrt{\epsilon^2 + \Delta^2}$.

Equation (8) is often referred to as ‘‘the rigid boundary condition’’. It corresponds to neglecting the inverse proximity effect as well as depairing effect in the leads due to a finite current density (see, e.g., review 14).

B. Saddle point: average Josephson current

We start the analysis of the σ -model (7) with the saddle-point approximation, which amounts to neglecting mesoscopic fluctuations and weak-localization corrections. The matrix Q_0 which extremizes the action solves the saddle-point equation:

$$\left[\epsilon \tau_3 + \sum_{i=L,R} \frac{G_i \delta}{4\pi G_Q} Q_i, Q_0 \right] = 0. \quad (9)$$

Equation (9) is nothing but the Usadel equation for the quasiclassical Green's function for a chaotic dot supplied by the Kupriyanov-Lukichev boundary conditions²⁶ at the tunnel interface. This equation can also be obtained with the help of Nazarov's ‘‘circuit theory’’.³³

The solution of Eq. (9) proportional to the unit matrix in the replica and spin spaces can be easily found:

$$Q_0 = (\tau_1 \cos \phi - \tau_2 \sin \phi) \sin \theta + \tau_3 \cos \theta, \quad (10)$$

where

$$\tan \theta(\epsilon) = \frac{\Delta E_g(\chi)}{\epsilon(\sqrt{\epsilon^2 + \Delta^2} + E_g)}, \quad (11a)$$

$$\tan \phi = \frac{G_R - G_L}{G_L + G_R} \tan \chi, \quad (11b)$$

and

$$E_g(\chi) = \frac{\delta}{4\pi G_Q} \sqrt{G_L^2 + G_R^2 + 2G_L G_R \cos \chi}, \quad (12)$$

with $E_g \equiv E_g(0)$. The pole of Q_0 located at imaginary ϵ is related to the minigap $E_*(\chi)$ in the density of states of the normal island.⁸ In the limiting cases,

$$E_*(\chi) = \begin{cases} E_g(\chi), & \Delta \gg E_g, \\ (\Delta/E_g) E_g(\chi), & \Delta \ll E_g, \end{cases} \quad (13)$$

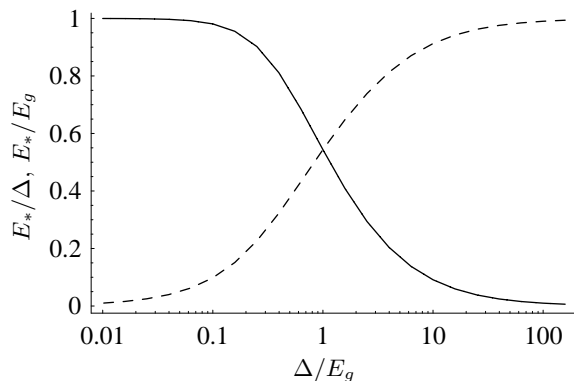


FIG. 1: The minigap E_* vs. Δ/E_g in a superconductor–quantum dot–superconductor Josephson junction with symmetric tunnel barriers. The two curves correspond to E_* in units of Δ (solid line) and in units of E_g (dashed line).

while in the intermediate region, $\Delta \sim E_g$, the dependence of E_* on χ is more complicated. In what follows, we will denote $E_* = E_*(0)$. Roughly speaking, $E_* \approx \min(\Delta, E_g)$, see Fig. 1.

The action at the saddle point is given by nS_0 , where n is the number of replicas and

$$S_0(\chi) = -\frac{2\pi}{\delta} \sum_{\epsilon} \omega_{\epsilon}(\chi), \quad (14)$$

with the summation over the fermion Matsubara energies $\epsilon_p = \pi(2p+1)kT$, and

$$\omega_{\epsilon}(\chi) = \frac{\sqrt{\epsilon^2(\sqrt{\epsilon^2 + \Delta^2} + E_g)^2 + \Delta^2 E_g(\chi)^2}}{\sqrt{\epsilon^2 + \Delta^2}}. \quad (15)$$

In the leading order in $G/G_Q \gg 1$, one can neglect weak localization and mesoscopic fluctuations effects (they will be studied in the next subsections). In this approximation, equivalent to the standard quasiclassical analysis, the Gaussian integral near the saddle point yields unity, and the average Josephson current can now be obtained from Eqs. (3)–(5) as $\langle I(\chi) \rangle_0 = (2ekT/\hbar)\partial S_0(\chi)/\partial\chi$, yielding

$$\langle I(\chi) \rangle_0 = \frac{\pi kT}{e} G E_g \sum_{\epsilon} \frac{\Delta^2 \sin \chi}{(\epsilon^2 + \Delta^2) \omega_{\epsilon}(\chi)}. \quad (16)$$

The result (16) is certainly not new. It had been obtained previously by a number of authors^{20,25–27}. Here we simply rederive this result for completeness.

Symmetric junction

The general expression (16) simplifies for symmetric barriers: $G_L = G_R = 2G$. In this case, $E_g(\chi) = E_g |\cos(\chi/2)|$ and $E_g = G\delta/\pi G_Q$.

At zero temperature (more precisely, $kT \ll E_*$), the average Josephson current is controlled by the ratio Δ/E_g .

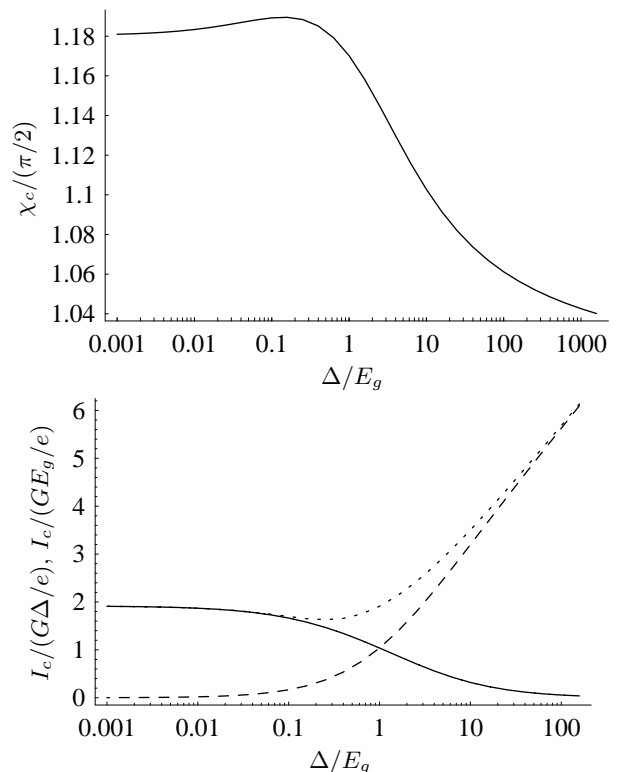


FIG. 2: Quasiclassical results for a superconductor–quantum dot–superconductor Josephson junction with symmetric tunnel barriers: (a) the critical phase χ_c (in units of $\pi/2$) vs. Δ/E_g at zero temperature; (b) the critical current I_c (solid line: in units of $G\Delta/e$, dashed line: in units of GE_g/e , dotted line: in units of GE_*/e) vs. Δ/E_g at zero temperature.

When $\Delta \ll E_g$, the Josephson relation is not sinusoidal:

$$\langle I(\chi) \rangle_0 = \frac{G\Delta}{e} \sin \chi \mathbf{K} \left(\sin \frac{\chi}{2} \right), \quad (17)$$

where $\mathbf{K}(x) = F(\pi/2, x)$ is the full elliptic integral of the first kind defined as in Ref. 34. The critical current $I_c \simeq 1.92G\Delta/e$ is achieved at a phase difference $\chi_c \simeq 1.18(\pi/2)$.

In the opposite limit, $\Delta \gg E_g$, the Josephson relation is close to sinusoidal:

$$\langle I(\chi) \rangle_0 \simeq \frac{GE_g}{e} \sin \chi \ln \left(\frac{2\Delta}{E_g(\chi)} \right), \quad (18)$$

with the critical current $I_c \simeq (GE_g/e) \ln(2\Delta/E_g)$ at a phase difference $\chi_c \simeq \pi/2$.

The crossover for the critical current and critical phase at zero temperature and arbitrary relation between Δ and E_g is illustrated in Fig. 2.

At temperature close to the critical temperature of the leads, T_c , the superconducting gap vanishes as $\Delta(T) \propto k[T_c(T_c - T)]^{1/2}$. Then for relevant energies $\epsilon \gtrsim kT \gg \Delta(T)$, Eq. (16) can be simplified, yielding a sinusoidal

Josephson relation with the critical current

$$I_c = \begin{cases} (\pi G \Delta^2 / 4ekT_c), & \Delta \ll E_g, \\ 7\zeta(3)GE_g\Delta^2 / 4e\pi^2k^2T_c^2, & \Delta \gg E_g, \end{cases} \quad (19)$$

where $\zeta(3) \approx 1.202$ is the Riemann zeta function.

At intermediate temperatures, $E_g \ll kT \ll kT_c$, we find $I_c = (GE_g/e) \ln(2\gamma\Delta/\pi kT)$, where $\gamma = e^C = 1.781\dots$ is the Euler constant, in agreement with Ref. 25–27.

C. Gaussian fluctuations near the saddle point

In this subsection we take Gaussian fluctuations near the saddle point into account. Since we will be interested in mesoscopic fluctuations of the Josephson current (see Sec. II E), we will have to consider the average $\langle Z_{\chi_1}^{n_1} Z_{\chi_2}^{n_2} \rangle$ of two partition functions calculated at different superconducting phases χ_1 and χ_2 . This average can also be expressed in terms of the σ -model:

$$\langle Z_{\chi_1}^{n_1} Z_{\chi_2}^{n_2} \rangle = \int \mathcal{D}Q e^{-S[Q]}, \quad (20)$$

where the only difference with the σ -model described in Sec. II A is that now Q becomes an $(n_1 + n_2) \times (n_1 + n_2)$ matrix in the replica space. Correspondingly, the superconducting Q -matrices in the terminals should be modified. Now they are diagonal in the replica space, having the superconducting phase difference χ_1 (resp. χ_2) in the n_1 first (resp. n_2 last) replicas. With these modification, the action of the σ -model has the same form (7).

At the saddle-point, the matrix Q_0 extremizing the action is diagonal in the energy and replica spaces. Its diagonal elements are given by Eqs. (10) and (11), where the phase χ is set to χ_1 (resp. χ_2) if $1 \leq a \leq n_1$ (resp. $n_1 < a \leq n_1 + n_2$), where a is a replica index.

In order to study fluctuations near this saddle point we write matrices close to Q_0 as

$$Q = U^\dagger \Lambda (1 + W + W^2/2 + \dots) U. \quad (21)$$

Here, the matrices Λ and U should be chosen in such a way that in the absence of fluctuations, at $W = 0$, Eq. (21) reduces to $U^\dagger \Lambda U = Q_0$. As usually, one has to require

$$\{\Lambda, W\} = 0, \quad (22a)$$

and impose the constraint following from Eq. (6):

$$\overline{W} = -W, \quad (22b)$$

and the requirement of convergency of the σ -model on the perturbative level:

$$W^\dagger = -W. \quad (22c)$$

The form of the parametrization (21) is standard, while the choice of the matrix Λ is a matter of convenience.

A possible choice could be the metallic saddle point,³¹ $\Lambda_M = \tau_3 \text{sign}(\epsilon)$ [the limit of Eq. (8) at $\epsilon \gg \Delta$]. Here we adopt an alternative choice proposed by Ostrovsky and Feigel'man³⁵:

$$\Lambda = \tau_1, \quad (23)$$

corresponding to the superconducting saddle point (8) at zero energy and $\chi = 0$. With this choice of Λ , the unitary matrix U in Eq. (21) is given by

$$U = e^{-i\tau_2(\pi/4 - \theta/2)} e^{-i\tau_3(\phi/2)}. \quad (24)$$

The choice of the parametrization with $\Lambda = \tau_1$ has two technical advantages: (i) the solution of the constraint (22a) is independent on energy, and (ii) the constraint (22b) can be easily resolved.

A general parametrization of the matrix W satisfying the constraint (22a) is given by:

$$W_{mn} = \tau_3 \hat{d}_{mn} + \tau_2 \hat{c}_{mn}, \quad (25)$$

where $m = (\epsilon, a)$ and $n = (\epsilon', b)$ encode both the energy and replica indices, and \hat{d}_{mn} and \hat{c}_{mn} are 2×2 matrices in the spin space which can be expanded in the Pauli matrices as

$$\hat{d} = d_0 + \mathbf{d}\boldsymbol{\sigma}, \quad \hat{c} = c_0 + \mathbf{c}\boldsymbol{\sigma}. \quad (26)$$

The variables d_0 and c_0 (\mathbf{d} and \mathbf{c}) will be referred to as singlet (triplet) modes. They play the same role as diffusons and Cooperons in a normal metal, describing soft diffusive excitations on top of an inhomogeneous proximity-induced state. Note that contrary to diffusive modes in a normal metal, these d - and c -modes are generally coupled in the presence of a supercurrent in the normal region, cf. Sec. III.

Equations (22b) and (22c) yield

$$d_0 = d_0^T = -d_0^\dagger, \quad \mathbf{d} = -\mathbf{d}^T = -\mathbf{d}^\dagger, \quad (27a)$$

$$c_0 = -c_0^T = -c_0^\dagger, \quad \mathbf{c} = \mathbf{c}^T = -\mathbf{c}^\dagger. \quad (27b)$$

Here, transposition acts in the replica and energy spaces. In terms of the matrix elements, Eqs. (27a), e.g., read:

$$(d_0)_{\epsilon, \epsilon'}^{ab} = (d_0)_{-\epsilon', -\epsilon}^{ba} = -(d_0^*)_{\epsilon', \epsilon}^{ba}, \quad (28a)$$

$$(d_i)_{\epsilon, \epsilon'}^{ab} = -(d_i)_{-\epsilon', -\epsilon}^{ba} = -(d_i^*)_{\epsilon', \epsilon}^{ba}. \quad (28b)$$

Independent integration variables for the singlet d_0 mode can be chosen, e.g., as:

$$(d_0)_{\epsilon, \epsilon'}^{ab} \in \mathbb{C}, \quad \text{if } a > b, \epsilon > 0,$$

$$(d_0)_{\epsilon, \epsilon'}^{aa} \in \mathbb{C}, \quad \text{if } \epsilon > |\epsilon'| > 0,$$

$$(d_0)_{\epsilon, -\epsilon}^{aa} \in \mathbb{C}, \quad \text{if } \epsilon > 0,$$

$$(d_0)_{\epsilon, \epsilon}^{aa} \in i\mathbb{R}, \quad \text{if } \epsilon > 0,$$

and analogously for the triplet $c_{i=1,2,3}$. Independent integration variables for the triplet $d_{i=1,2,3}$ modes can be

chosen, e.g., as:

$$\begin{aligned} (d_i)_{\epsilon, \epsilon'}^{ab} &\in \mathbb{C}, & \text{if } a > b, \epsilon > 0, \\ (d_i)_{\epsilon, \epsilon'}^{aa} &\in \mathbb{C}, & \text{if } \epsilon > |\epsilon'| > 0, \\ (d_i)_{\epsilon, \epsilon}^{aa} &\in i\mathbb{R}, & \text{if } \epsilon > 0, \end{aligned}$$

and analogously for the singlet c_0 .

Expanding the action in the Gaussian approximation over fluctuations near the saddle point, one finds in general:

$$S^{(2)} = \frac{\pi}{\delta} \sum_{mn} \sum_{i=0}^3 (d_i^* \ c_i^*)_{mn} \hat{A}_{mn} \begin{pmatrix} d_i \\ c_i \end{pmatrix}_{mn}, \quad (29)$$

where \hat{A}_{mn} is a symmetric [it can be symmetrized using relations (27)] matrix in the (d, c) -space with the simple block structure in the replica space:

$$\hat{A}_{\epsilon\epsilon'}^{ab} = \begin{cases} A_{\epsilon\epsilon'}^{X^1X^1}, & \text{if } a, b \leq n_1, \\ A_{\epsilon\epsilon'}^{X^1X^2}, & \text{if } a \leq n_1 < b, \\ A_{\epsilon\epsilon'}^{X^2X^1}, & \text{if } b \leq n_1 < a, \\ A_{\epsilon\epsilon'}^{X^2X^2}, & \text{if } n_1 < a, b. \end{cases} \quad (30)$$

The matrix \hat{A} does not depend on the spin index i since the spin is conserved. Such a dependence will arise if one takes magnetic impurities or spin-orbit interaction in the normal region into account.

Due to the absence of the $(d_i)_{\epsilon, -\epsilon}^{aa}$ and $(c_0)_{\epsilon, -\epsilon}^{aa}$ modes, the matrix $\hat{A}_{\epsilon, -\epsilon}^{aa}$ should be diagonal in the (d, c) -space:

$$A_{\epsilon, -\epsilon}^{XX} = \begin{pmatrix} (A_{\epsilon, -\epsilon}^{XX})^{dd} & 0 \\ 0 & (A_{\epsilon, -\epsilon}^{XX})^{cc} \end{pmatrix}. \quad (31)$$

We will see below that this is indeed the case [cf. Eqs. (35) and (62)].

Integration over independent variables of the d and c modes gives the fluctuation determinant:

$$\langle Z_{\chi_1}^{n_1} Z_{\chi_2}^{n_2} \rangle = \mathcal{M} e^{-n_1 \tilde{S}_0(\chi_1) - n_2 \tilde{S}_0(\chi_2)}, \quad (32)$$

where $\tilde{S}_0(\chi)$ contains the WL correction:

$$\tilde{S}_0(\chi) = S_0(\chi) - \frac{1}{2} \sum_{\epsilon} \text{tr} \ln \frac{(A_{\epsilon, -\epsilon}^{XX})^{dd}}{(A_{\epsilon, -\epsilon}^{XX})^{cc}} \quad (33)$$

[we write this expression in the most general way assuming that $(A_{\epsilon, -\epsilon}^{XX})^{dd}$ and $(A_{\epsilon, -\epsilon}^{XX})^{cc}$ might be operators, as in Sec. III; for a chaotic dot considered in this section, the trace in Eq. (33) can be omitted], whereas the prefactor \mathcal{M} accounts for mesoscopic fluctuations:

$$\mathcal{M} = \prod_{\epsilon, \epsilon'} \frac{1}{(\det A_{\epsilon\epsilon'}^{X^1X^1})^{n_1^2} (\det A_{\epsilon\epsilon'}^{X^1X^2})^{2n_1n_2} (\det A_{\epsilon\epsilon'}^{X^2X^2})^{n_2^2}}. \quad (34)$$

In Eq. (34), the product over ϵ and ϵ' should be taken over all Matsubara energies and we have omitted the factors

which are equal to 1 in the replica limit $n_{1,2} \rightarrow 0$ and do not depend on $\chi_{1,2}$.

For a superconductor–quantum dot–superconductor junction considered in this Section, the matrix \hat{A} can be easily found by expanding the action (7) in W with the help of Eqs. (21)–(25):

$$A_{\epsilon\epsilon'}^{XX'} = \frac{\omega_{\epsilon}(\chi) + \omega_{\epsilon'}(\chi')}{2} \hat{\Sigma}_0, \quad (35)$$

where $\omega_{\epsilon}(\chi)$ is defined in Eq. (15), and $\hat{\Sigma}_0$ is the identity matrix in the (d, c) -space.

The weak localization correction to the Josephson current and its mesoscopic fluctuations are discussed in the next Subsections.

D. Weak localization correction

The weak localization correction to the Josephson current, $\Delta_{\text{WL}} I(\chi) \equiv \langle I(\chi) \rangle - \langle I(\chi) \rangle_0$, can be found with the help of Eqs. (3), (4), (32) and (33):

$$\Delta_{\text{WL}} I(\chi) = -\frac{ekT}{\hbar} \frac{\partial}{\partial \chi} \sum_{\epsilon} \text{tr} \ln \frac{(A_{\epsilon, -\epsilon}^{XX})^{dd}}{(A_{\epsilon, -\epsilon}^{XX})^{cc}}. \quad (36)$$

Since for a superconductor–quantum dot–superconductor junction, the matrix \hat{A} [see Eq. (35)] acts as a unit matrix in the (d, c) -space, there is no weak localization correction to the Josephson current.

Note that there is no weak localization correction to the conductance of a normal metal–quantum dot–normal metal junction in the lowest order in the tunnel barriers either^{15,36}.

E. Mesoscopic fluctuations

With the help of the replica trick and relation (3), the current-current correlation function can be expressed as

$$\langle I(\chi_1) I(\chi_2) \rangle = \left(\frac{2ekT}{\hbar} \right)^2 \frac{\partial^2}{\partial \chi_1 \partial \chi_2} \lim_{n_1, n_2 \rightarrow 0} \frac{\langle Z_{\chi_1}^{n_1} Z_{\chi_2}^{n_2} \rangle}{n_1 n_2}. \quad (37)$$

Making use of Eqs. (32) and (34), we get the general expression for the cumulant $\langle\langle I(\chi_1) I(\chi_2) \rangle\rangle \equiv \langle I(\chi_1) I(\chi_2) \rangle - \langle I(\chi_1) \rangle \langle I(\chi_2) \rangle$:

$$\langle\langle I(\chi_1) I(\chi_2) \rangle\rangle = -8 \left(\frac{ekT}{\hbar} \right)^2 \frac{\partial^2}{\partial \chi_1 \partial \chi_2} \sum_{\epsilon\epsilon'} \text{tr} \ln A_{\epsilon\epsilon'}^{X^1X^2}. \quad (38)$$

Since $A_{\epsilon\epsilon'}^{X^1X^2}$ given by Eq. (35) appears to be diagonal in the (d, c) -space, evaluation of Eq. (38) for the quantum dot geometry is trivial and we get:

$$\begin{aligned} \langle\langle I(\chi_1) I(\chi_2) \rangle\rangle &= \left(\frac{4ekT}{\hbar} \right)^2 \sum_{\epsilon\epsilon'} \frac{1}{[\omega_{\epsilon}(\chi_1) + \omega_{\epsilon'}(\chi_2)]^2} \frac{\partial \omega_{\epsilon}}{\partial \chi_1} \frac{\partial \omega_{\epsilon'}}{\partial \chi_2}. \quad (39) \end{aligned}$$

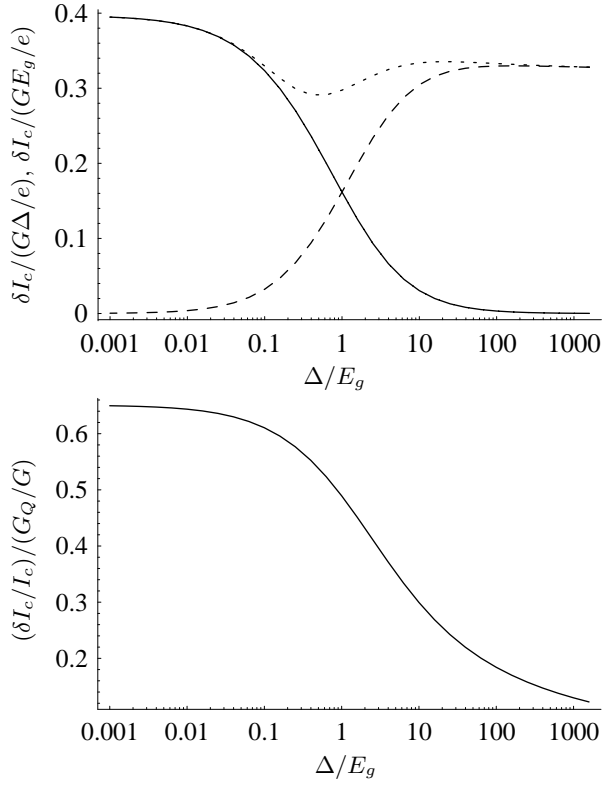


FIG. 3: (a) Mesoscopic fluctuations of the critical current, $\delta I_c = (\text{var } I_c)^{1/2}$ (solid line: in units of $e\Delta/\hbar$, dashed line: in units of eE_g/\hbar , dotted line: in units of eE_*/\hbar) vs. Δ/E_g at zero temperature. (b) The ratio $G\delta I_c/G_Q I_c$ vs. Δ/E_g at zero temperature.

In the limits $T = 0$ and $\Delta \ll E_g$, Eq. (39) had been recently derived by Micklitz²⁰ using the supersymmetric σ -model approach.

As shown in Ref. 37, mesoscopic fluctuations of the *critical* current, δI_c , can be obtained as $\delta I_c = \delta I(\chi_c)$.

Symmetric junction

We consider now symmetric junctions.

At zero temperature, we find:

$$\delta I_c = \begin{cases} 0.396(e\Delta/\hbar), & \text{if } \Delta \ll E_g, \\ eE_g/\pi\hbar, & \text{if } E_g \ll \Delta, \end{cases} \quad (40)$$

while the result for an arbitrary ratio Δ/E_g is plotted in Fig. 3.

A peculiar feature of the $T = 0$ mesoscopic fluctuations given by Eq. (39) is a finite limit at $\chi \rightarrow \pi$:

$$\delta I(\pi) = \frac{\sqrt{2}e}{\pi\hbar} \frac{\Delta E_g}{\Delta + E_g} \sim \frac{eE_*}{\hbar}, \quad (41)$$

while the Josephson current must vanish exactly at $\chi = \pi$.^{20,37} This is related to the breakdown of the Gaus-

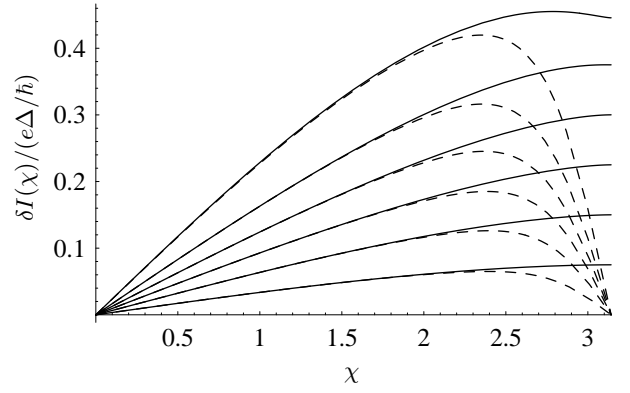


FIG. 4: Mesoscopic fluctuations of the Josephson current, $\delta I(\chi)$ vs. phase χ at zero temperature (solid line) and at temperature $kT = E_*/10$ (dashed line). The curves are plotted for different ratios Δ/E_g : 0 (top), 0.2, 0.5, 1, 2, 5 (bottom).

sian treatment of fluctuations at $\chi \rightarrow \pi$. A more careful analysis of the general nonlinear action (7) should restore the exact relation $I(\pi) = 0$, resulting in vanishing fluctuations for $\chi \rightarrow \pi$.²⁰ At a small temperature, $\delta I(\pi) = 0$, and the Josephson current decreases from its typical value (41) to 0 in the small phase range $|\chi - \pi| \lesssim kT/E_*$, see Fig. 4.

Close to the critical temperature, T_c , when $\Delta(T) \rightarrow 0$, we find

$$\delta I_c^2 = \left(\frac{2ekT}{\hbar} \Delta^2(T) E_g^2 \right)^2 \times \sum_{\epsilon, \epsilon' > 0} \frac{1}{\epsilon^2 \epsilon'^2 (\epsilon + \epsilon' + 2E_g)^2 (\epsilon + E_g) (\epsilon' + E_g)}. \quad (42)$$

Thus,

$$\delta I_c = \begin{cases} (e\Delta^2(T)/8\hbar kT_c), & \text{if } kT_c \ll E_g, \\ 0.010e\Delta^2(T)E_g^2/\hbar k^3 T_c^3, & \text{if } E_g \ll kT_c. \end{cases} \quad (43)$$

At intermediate temperatures such that $E_g \ll kT \ll kT_c$, we find

$$\delta I_c^2 = \left(\frac{2ekT}{\hbar} E_g^2 \right)^2 \sum_{\epsilon, \epsilon' > 0} \frac{1}{\epsilon \epsilon' (\epsilon + \epsilon')^2}. \quad (44)$$

Thus, $\delta I_c \simeq 0.12(eE_g^2/\hbar kT)$. This result was also obtained by means of the fourth order perturbation theory in the tunnel Hamiltonian connecting the wire to the leads, plus random matrix theory on the statistics of eigenstates in the lead.³⁸

F. Summary of results

The results of our study are summarized in Table I. We note that, quite generally, the critical current at low temperatures is related to the minigap in the dot at $\chi =$

TABLE I: Summary of results for a quantum dot contacted symmetrically to superconducting leads ($G_L = G_R = 2G$).

	$\chi_c/(\pi/2)$	eI_c/G	$\Delta_{\text{WL}}I(\chi)$	$\hbar\delta I_c/e$	$g\delta I_c/I_c$
$\Delta \ll E_g, T = 0$	1.18	$1.92\Delta^{[26,27]}$	0	$0.396\Delta^{[20]}$	0.648
$E_g \ll \Delta, T = 0$	1	$E_g \ln(2\Delta/E_g)^{[27]}$	0	E_g/π	$1/\ln(2\Delta/E_g)$
arbitrary $E_g/\Delta, T = 0$	Fig. 2(a)	Fig. 2(b)	0	Fig. 3(a)	Fig. 3(b)
$kT \lesssim kT_c \ll E_g$	1	$\pi\Delta^2(T)/4kT_c^{[26]}$	0	$\Delta^2(T)/8kT_c$	1/2
$E_g \ll kT \lesssim kT_c$	1	$0.213E_g\Delta^2(T)/(kT_c)^2^{[26]}$	0	$0.010\Delta^2(T)E_g^2/(kT_c)^3$	$0.15E_g/kT_c$
$E_g \ll kT \ll kT_c$	1	$E_g \ln(2\gamma\Delta/\pi kT)^{[25-27]}$	0	$0.12E_g^2/kT$	$0.38E_g/[kT \ln(2\gamma\Delta/\pi kT)]$

Here, $g = G/G_Q$, $\Delta(T) = [(8\pi^2/7\zeta(3))k^2T_c(T_c - T)]^{1/2}$ and $\gamma = 1.781\dots$

0, $E_* \sim \min(E_g, \Delta)$, through an Ambegaokar-Baratoff like formula: $I_c \sim GE_*/e$, where G is the normal-state conductance of the system (up to a logarithmic factor for $E_g \ll \Delta$).

In a normal metallic double-barrier structure, conductance fluctuations are “universal”: $\delta G = G_Q/2$, while weak localization corrections vanish at infinitely small mean level spacing in the dot^{15,36}.

In an S-QD-S junction, we find that the WL correction to the Josephson current also vanishes, while the amplitude of mesoscopic fluctuations can be estimated as $\delta I_c/I_c \sim \delta G/G$, provided $kT_c \ll E_g$. In the opposite limit, for poorly conducting barriers, mesoscopic fluctuations are additionally suppressed.

Note that in the limit $kT \lesssim kT_c \ll E_g$, we have $\delta I_c/I_c = \delta G/G$. This should be attributed to the fact that in this limit the Josephson relation becomes sinusoidal and proportional to the conductance of the system. Indeed, using Eq. (15) from Ref. 18 with $\Delta(T) \ll kT$, we find $I(\chi) = I_c \sin \chi$, where the critical current is proportional to the exact conductance before disorder averaging: $I_c = (e\Delta^2(T)/4\hbar kT) \sum_n T_n = \pi\Delta^2(T)G/4ekT$.

III. SUPERCONDUCTOR-NORMAL METAL-SUPERCONDUCTOR JUNCTIONS

We turn now to the case of a diffusive metallic wire connected to superconducting leads by transparent interfaces (the interface resistances are much lower than the resistance of the wire in the normal state).

Proximity effect in such a geometry can be described by the diffusive replica σ -model with the action^{21,31}

$$S[Q] = \frac{\pi\nu}{8} \int d\mathbf{r} \text{tr} [D(\nabla Q)^2 - 4\epsilon\tau_3 Q], \quad (45)$$

where D is the diffusion coefficient. At the boundaries with superconductors, we require that Q matches with the Q_i matrices in the leads given by Eq. (8).

In this Section we concentrate on a quasi-one-dimensional geometry, when the length of the wire, L , much exceeds its transverse dimensions. Then, the spatial dependence of Q is reduced to the dependence on the coordinate x along the wire, which will be measured in

units of L . The action (45) can be written as

$$S[Q] = \frac{G_N}{16G_Q} \int_{-1/2}^{1/2} dx \text{tr} [(\nabla Q)^2 - 4\epsilon\tau_3 Q], \quad (46)$$

where $G_N = 2\pi G_Q E_T/\delta$ is the normal-state conductance of the wire, and $\epsilon = \epsilon/E_T$ stands for Matsubara energies measured in units of the Thouless energy, $E_T = \hbar D/L^2$.

Following the same line as in Sec. II, we derive the quasiclassical Josephson relation as the saddle point of the action (46) in Sec. III A. We find that the amplitude of the critical current is controlled by the ratio between Δ and E_T . Then, we express mesoscopic fluctuations and WL correction to the Josephson current in terms of Gaussian fluctuations in the vicinity of the non-uniform saddle point in Sec. III B. Results are summarized in Sec. III C.

A. Josephson relation

At the saddle point, the matrix $Q_0(x)$ which extremizes the action (46) solves the Usadel equation:

$$-\nabla(Q_0\nabla Q_0) + \epsilon[\hat{\tau}_3, Q_0] = 0. \quad (47)$$

With the parametrization (10), this equation can be reduced to two differential equations:

$$\nabla(\sin^2\theta\nabla\phi) = 0, \quad (48a)$$

$$\nabla^2\theta - 2\epsilon\sin\theta - (\nabla\phi)^2\sin\theta\cos\theta = 0, \quad (48b)$$

with the boundary conditions $\theta(\pm 1/2) = \theta_s$ and $\phi(\pm 1/2) = \pm\chi/2$. The Usadel angles at energies $\pm\epsilon$ are related by the symmetries:

$$\theta_{-\epsilon} = \pi - \theta_\epsilon, \quad \phi_{-\epsilon} = \phi_\epsilon. \quad (49)$$

According to Eq. (48a), $J = \sin^2\theta\nabla\phi$ (usually referred to as the spectral current) is constant along the wire. Integrating then Eq. (48b), we obtain:

$$(\nabla\theta)^2 = 4\epsilon(\cos\theta(0) - \cos\theta) + \frac{J^2}{\sin^2\theta(0)} - \frac{J^2}{\sin^2\theta}. \quad (50)$$

This last equation can be solved in quadratures, the implicit solution being given in terms of elliptic integrals.

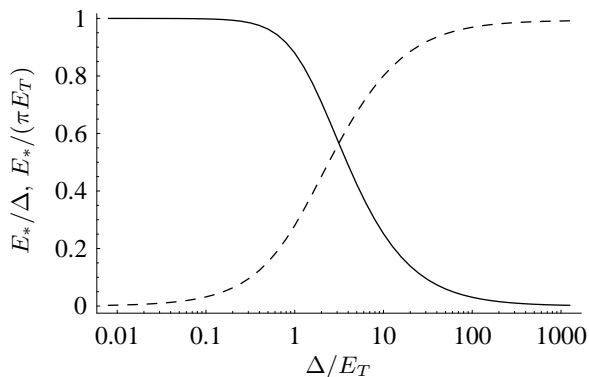


FIG. 5: The minigap E_* induced in the normal wire at $\chi = 0$ (solid line: in units of Δ , dashed line: in units of πE_T) vs. Δ/E_T .

Its form is rather cumbersome and can be found in Appendix A. In a general case, J and $\theta(0)$ at given boundary conditions can be found only numerically. Note however that their determination requires solution of only an algebraic rather than differential equation.

Equation (50) can be used to determine the minigap E_* induced in the normal region due to the proximity effect. To this end, one has to perform analytic continuation $\epsilon \rightarrow -iE$, and search for the energy E_* when $\cos \theta$ first acquires a finite real part, indicating a nonzero density of states above E_* . Determination of the minigap simplifies for $\chi = 0$. To solve the Usadel equation we introduce then $\theta = \pi/2 + i\psi$ and get the relation between E and the value $\psi(0)$ at the center of the wire:

$$\sqrt{\frac{E}{E_T}} = \int_{\text{arctanh}(E/\Delta)}^{\psi(0)} \frac{d\psi}{\sqrt{\sinh \psi(0) - \sinh \psi}}. \quad (51)$$

Equation (51) establishes a relation between E and $\psi(0)$. The value of E_* should be determined from the condition that Eq. (51) ceases to have real solutions for $\psi(0)$. For short wires ($\Delta \ll E_T$), $E_* \approx \Delta$, whereas for long wires ($\Delta \gg E_T$), $E_* \approx 3.122E_T$,^{39,40} in accordance with the general relation $E_* \sim \min(E_T, \Delta)$. The dependence of E_* on Δ/E_T is shown in Fig. 5.

The action at the saddle point $Q_0(x)$ is given by nS_0 , where

$$S_0 = \frac{G_N}{4G_Q} \sum_{\epsilon} \int dx [(\nabla\theta)^2 + (\nabla\phi)^2 \sin^2 \theta - 4\epsilon \cos \theta], \quad (52)$$

Taking the derivative with respect to χ , integrating by parts, and using the boundary conditions at $x = \pm 1/2$ we get $\partial_{\chi} S_0 = (G_N/2G_Q) \sum_{\epsilon} J$, yielding the quasiclassical expression for the supercurrent:

$$\langle I(\chi) \rangle_0 = \pi kT \frac{G_N}{e} \sum_{\epsilon} J. \quad (53)$$

Below, we evaluate the current (53) in different cases.

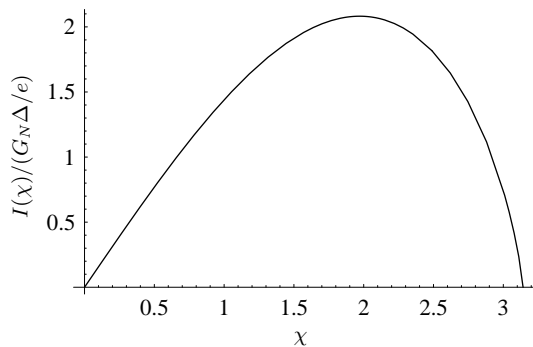


FIG. 6: Josephson relation $I(\chi)$ (in units of $G_N\Delta/e$) for a short wire at zero temperature.

1. Short wire at zero temperature

The critical current for a short diffusive wire ($E_T \gg \Delta$) has been known for a long time.¹¹ In this case, the term proportional to ϵ in Eq. (48b) can be neglected, and the Usadel equation can be solved exactly:

$$\theta(x) = \arccos \left[\cos \theta(0) \cos \frac{Jx}{\sin \theta(0)} \right], \quad (54)$$

where

$$\sin \theta(0) = \frac{\sin \theta_s \cos \frac{\chi}{2}}{\sqrt{1 - \sin^2 \theta_s \sin^2 \frac{\chi}{2}}}, \quad (55a)$$

$$J = 2 \sin \theta(0) \arcsin \left(\sin \theta_s \sin \frac{\chi}{2} \right). \quad (55b)$$

Calculating the supercurrent with the help of Eq. (53) at $T = 0$ we get¹¹

$$I(\chi) = \frac{\pi G_N \Delta}{e} \cos \frac{\chi}{2} \text{arctanh} \left(\sin \frac{\chi}{2} \right). \quad (56)$$

The Josephson relation is nonsinusoidal, see Fig. 6. The critical current $I_c = 2.082G_N\Delta/e$ is achieved at the critical phase $\chi_c = 1.255(\pi/2)$.

2. Arbitrary wire at temperature close to T_c

At temperatures close to the critical temperature in the leads, T_c , the superconducting gap Δ in the leads is small: $\Delta(T) = [(8\pi^2/7\zeta(3))k^2T_c(T_c - T)]^{1/2} \ll kT$. Thus, at relevant energies $\epsilon \gtrsim kT \gg \Delta$, the anomalous (Gor'kov) component of the Green function is small, and the Usadel equation (48b) can be linearized with respect to $\sin \theta$. Its solution has the form

$$\begin{aligned} \sin \theta(x) e^{i\phi(x)} &= \frac{\Delta}{|\epsilon|} e^{-i\frac{\chi}{2}} \frac{\sinh \kappa(\frac{1}{2} - x)}{\sinh \kappa} \\ &+ \frac{\Delta}{|\epsilon|} e^{i\frac{\chi}{2}} \frac{\sinh \kappa(\frac{1}{2} + x)}{\sinh \kappa}, \end{aligned} \quad (57)$$

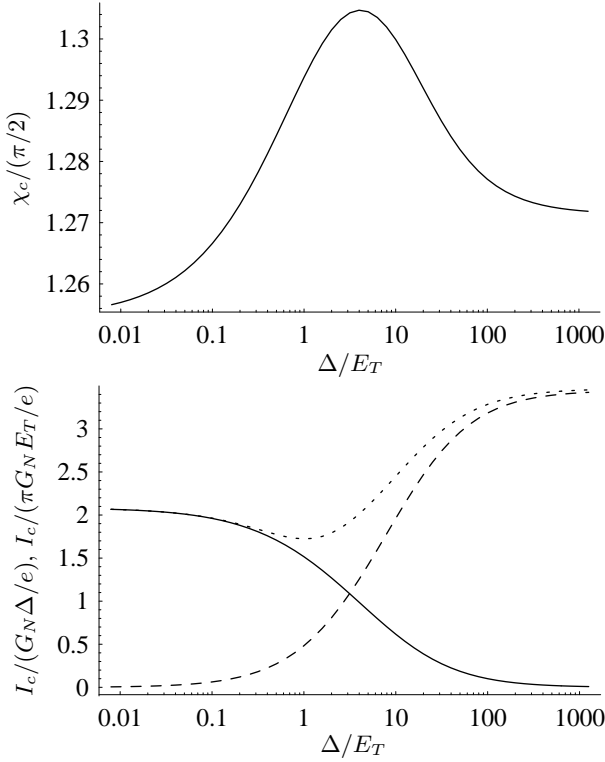


FIG. 7: (a) The critical phase χ_c (in units of $\pi/2$) vs. Δ/E_T at zero temperature. (b) The critical current I_c (solid line: in units of $G_N \Delta/e$, dashed line: in units of $\pi G_N E_T/e$, dotted line: in units of $G_N E_*/e$) vs. Δ/E_T at zero temperature.

where $\kappa = \sqrt{2|\varepsilon|} = \sqrt{2|\varepsilon|/E_T}$. Calculating the spectral current with the help of Eqs. (D1) and (D2), we get

$$J = \frac{\Delta^2}{\varepsilon^2} \frac{\kappa}{\sinh \kappa} \sin \chi. \quad (58)$$

Close to T_c , junctions are classified as short or long depending on the ratio between kT_c and E_T . For short junctions [$\Delta(T) \ll kT \lesssim kT_c \ll E_T$], the supercurrent is given by:

$$I(\chi) = \frac{\pi G_N \Delta^2}{4e kT} \sin \chi. \quad (59)$$

For long junctions [$\Delta(T), E_T \ll kT \lesssim kT_c$], the supercurrent is exponentially suppressed:

$$I(\chi) \simeq \frac{8G_N}{e} \frac{\Delta^2}{\sqrt{2\pi kT E_T}} \exp\left(-\sqrt{\frac{2\pi kT}{E_T}}\right) \sin \chi. \quad (60)$$

In both cases the Josephson relation is sinusoidal.

3. Arbitrary wire at zero temperature

At $T = 0$ the Josephson relation $I(\chi)$ depends only on the ratio between Δ and E_T . Short junctions were

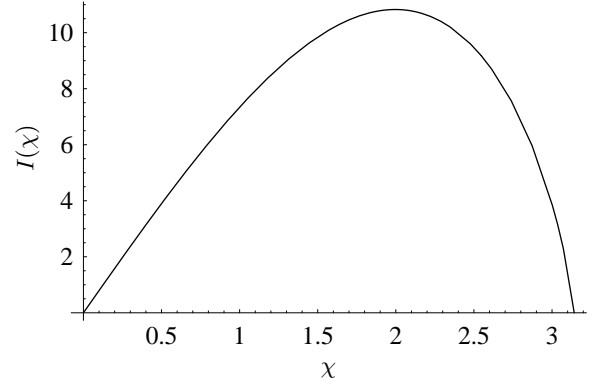


FIG. 8: Josephson relation $I(\chi)$ (in units of $G_N E_T/e$) for a long wire at zero temperature.

considered in Sec. III A 1. For arbitrary Δ/E_T , the critical current and critical phase obtained numerically are shown in Fig. 7.¹³

Specifically, for long junctions ($E_T \ll \Delta$) the Josephson relation is still highly nonsinusoidal (see Fig. 8), with the critical current $I_c = 10.83 G_N E_T/e$ achieved at the critical phase $\chi_c = 1.271(\pi/2)$.¹³

B. Mesoscopic fluctuations and weak localization correction

Fluctuations near the saddle point $Q_0(x)$ can be parametrized using Eqs. (21), (24) and (25). Substituting these expressions into the action (46) and expanding to the second order in the modes $d(x)$ and $c(x)$, we get similar to Eq. (29):

$$S^{(2)} = \frac{G_N}{4G_Q} \int dx \sum_{mn} \sum_{i=0}^3 \left(d_i^* \ c_i^* \right)_{mn} \hat{A}_{mn} \begin{pmatrix} d_i \\ c_i \end{pmatrix}_{mn}. \quad (61)$$

The form of the operator $\hat{A}(x)$ is quite cumbersome, see Eq. (B2) in Appendix B. Apart from the second derivative with respect to x it contains also the first derivative. The latter can be eliminated by a proper unitary transformation [Eq. (B5)] mixing the d and c components of fluctuations. After such a rotation the matrix \hat{A} acquires the form⁴¹

$$\hat{A}_{mn}(x) = -\nabla^2 + \alpha_{mn} + \rho_{mn} \cos(\eta_m + \eta_n) \hat{\Sigma}_3 + \rho_{mn} \sin(\eta_m + \eta_n) \hat{\Sigma}_1, \quad (62)$$

where

$$\alpha_{mn} = \varepsilon_m \cos \theta_m - \frac{1}{4} [(\nabla \theta_m)^2 + (\sin \theta_m \nabla \phi_m)^2] + \varepsilon_n \cos \theta_n - \frac{1}{4} [(\nabla \theta_n)^2 + (\sin \theta_n \nabla \phi_n)^2], \quad (63)$$

$$\rho_{mn} = \frac{1}{2} \sqrt{(\nabla \theta_m)^2 + (\sin \theta_m \nabla \phi_m)^2} \times \sqrt{(\nabla \theta_n)^2 + (\sin \theta_n \nabla \phi_n)^2}, \quad (64)$$

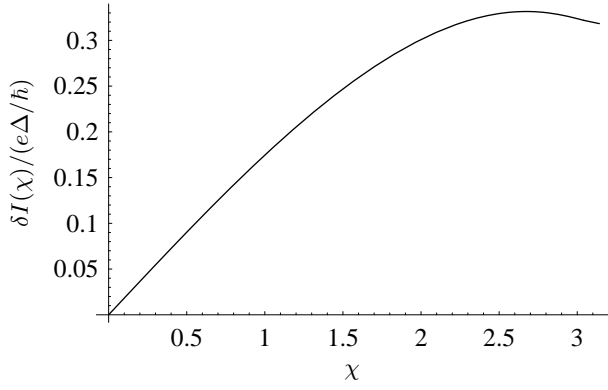


FIG. 9: Mesoscopic fluctuations $\delta I(\chi)$ (in units of $e\Delta/\hbar$) for a short wire at $T = 0$.

and the odd function $\eta_m(x)$ can be obtained by integrating the relation

$$\nabla\eta_m = -\frac{2\varepsilon_m J_m}{(\nabla\theta_m)^2 + (\sin\theta_m \nabla\phi_m)^2}. \quad (65)$$

Once the operator \hat{A} is known, one can use the general Eqs. (36) and (38) to calculate the weak localization correction and mesoscopic fluctuations of the Josephson current. The only difference compared to the S-QD-S case is that now $\hat{A}(x)$ is an operator in the real space, and the determinant should be calculated with respect to spacial coordinates as well. In a general situation, for arbitrary Δ/E_T and temperatures, this can be done only numerically, following the procedure outlined in Appendix A.

Several cases where a simple form of the operator $\hat{A}(x)$ allows for analytic solution are discussed below. In Sec. III B 3, we present the results of numeric solution for an arbitrary Δ/E_T at zero temperature.

1. Short wire

We start with the simplest case of a short wire, $\Delta \ll E_T$. This limit was analyzed previously in Refs. 16 and 17 using the scattering-matrix approach to the Josephson current.¹⁸

For short wires, the term proportional to ε in the Usadel equation can be neglected. Then, according to Eq. (50), $(\nabla\theta_m)^2 + (\sin\theta_m \nabla\phi_m)^2 = 4C_m^2$, where $C_m = J_m/2 \sin\theta_m(0)$ is constant in the wire. With the same accuracy, Eq. (65) guaranties that $\eta_m(x) = 0$. As a result, the operator \hat{A} in Eq. (62) becomes diagonal in the (d, c) -space, with its diagonal elements being diffusion operators:

$$\hat{A}_{mn} = \begin{pmatrix} -\nabla^2 - (C_m - C_n)^2 & 0 \\ 0 & -\nabla^2 - (C_m + C_n)^2 \end{pmatrix}.$$

Since fluctuations must vanish in the reservoirs, the eigenvalues of $-\nabla^2$ are $\pi^2 p^2$ ($p = 1, 2, \dots$), and the de-

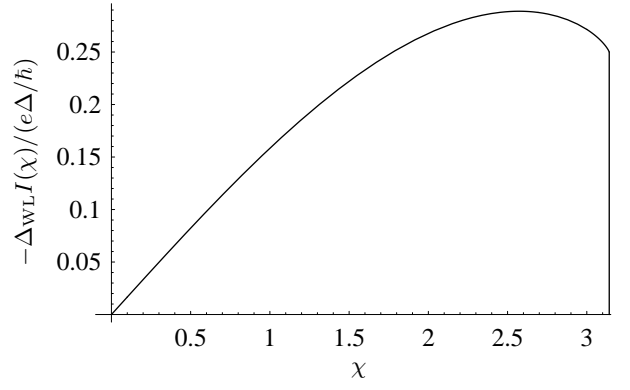


FIG. 10: Weak localization correction $-\Delta_{\text{WL}}I(\chi)$ (in units of $e\Delta/\hbar$) for a short wire at $T = 0$.

terminant of $A_{\varepsilon\varepsilon'}^{\chi_1\chi_2}$ involved in Eq. (38) can be readily obtained. As a result, the current-current correlation function acquires the form

$$\begin{aligned} \langle\langle I(\chi)I(\chi') \rangle\rangle &= -8 \left(\frac{ekT}{\hbar} \right)^2 \\ &\times \frac{\partial^2}{\partial\chi\partial\chi'} \sum_{\varepsilon\varepsilon'} \ln \frac{\sin(C - C')}{C - C'} \frac{\sin(C + C')}{C + C'}, \end{aligned} \quad (66)$$

where $C = \arcsin[(\Delta/\sqrt{\Delta^2 + \varepsilon^2}) \sin(\chi/2)]$ and C' is given by the same expression with $\varepsilon \rightarrow \varepsilon'$ and $\chi \rightarrow \chi'$.

At zero temperature, the sums over Matsubara energies reduce to integrals, and our expression for $\delta I^2(\chi) = \langle\langle I^2(\chi) \rangle\rangle = \text{var } I(\chi)$ becomes equivalent to the result of Refs. 16 and 17. The equivalence is explicitly demonstrated in Appendix C. For small χ , we have an expansion in powers of $\sin^2(\chi/2)$:

$$\delta I^2(\chi) = \left(\frac{e\Delta}{\hbar} \right)^2 \frac{\sin^2 \chi}{30} \left(1 + \frac{62}{63} \sin^2 \frac{\chi}{2} + \dots \right). \quad (67)$$

The whole curve $\delta I(\chi)$ at $T = 0$ is plotted in Fig. 9. Mesoscopic fluctuations of the critical current, $\delta I_c = \delta I(\chi_c)$, are characterized by $\delta I_c = 0.30e\Delta/\hbar$.^{16,17}

At zero temperature, the magnitude of mesoscopic fluctuations remains finite at $\chi = \pi$, $\delta I(\pi) = e\Delta/\pi\hbar$, contradicting the general symmetry requirement of vanishing $I(\chi)$.^{20,37} This is related to the breakdown of the Gaussian treatment of fluctuations at $\chi \rightarrow \pi$. A more careful analysis of the general nonlinear action (46) should restore the exact relation $I(\pi) = 0$, resulting in vanishing fluctuations for $\chi \rightarrow \pi$.²⁰ The region where the exact treatment should modify the result obtained in the Gaussian approximation can be estimated as $|\chi - \pi| \lesssim G_Q/G_N \ll 1$. Finite temperatures render $\delta I(\pi) = 0$, and shrink the region of strong non-Gaussian fluctuations near $\chi = \pi$, which disappears at $kT \gg (G_Q/G_N)|\chi - \pi|\Delta$.

The weak localization correction can be evaluated with the help of Eq. (36). Here, only c -modes contribute to

the result, and

$$\Delta_{\text{WL}}I(\chi) = \frac{ekT}{\hbar} \frac{\partial}{\partial \chi} \sum_{\epsilon} \ln \frac{\sin 2C}{2C}. \quad (68)$$

At zero temperature, we obtain:

$$\Delta_{\text{WL}}I(\chi) = -\frac{e\Delta}{6\hbar} \sin \chi \left(1 + \frac{7}{15} \sin^2 \frac{\chi}{2} + \dots \right). \quad (69)$$

in agreement with Eq. (3.33) of Ref. 16. The whole dependence $\Delta_{\text{WL}}I(\chi)$ at $T = 0$ is shown in Fig. 10. The WL correction to the critical current is $\Delta_{\text{WL}}I_c = -0.266e\Delta/\hbar$.

At zero temperature, the WL correction (68) is discontinuous at $\chi = \pi$: $\Delta_{\text{WL}}I(\pi \mp 0) = \mp e\Delta/4\hbar$, which is an artefact of the Gaussian approximation employed. The situation here is completely analogous to the situation with mesoscopic fluctuations discussed above.

2. Arbitrary wire at temperatures close to T_c

In Sec. III A 2 we have seen that calculation of the quasiclassical Josephson current simplifies at temperatures close to T_c . The same occurs for mesoscopic fluctuations and WL correction. In order to calculate them, we decompose the operator $\hat{A} = \hat{A}_0 + \hat{V}$ in Eq. (62) into a sum of the diffusion operator in the normal state, $\hat{A}_0 = -\nabla^2 + |\varepsilon_1| + |\varepsilon_2|$, and the perturbation $\hat{V} = \mathcal{O}(\Delta^2)$. Expanding $\text{tr} \ln \hat{A}$ in powers of \hat{V} we rewrite Eqs. (36) and (38) as

$$\begin{aligned} \Delta_{\text{WL}}I(\chi) &= -\frac{ekT}{\hbar} \frac{\partial}{\partial \chi} \sum_{\epsilon} \text{Tr} G \hat{\Sigma}_3 V_{\epsilon, -\epsilon}^{\chi\chi}, \quad (70) \\ \langle\langle I(\chi_1)I(\chi_2) \rangle\rangle &= 4 \left(\frac{ekT}{\hbar} \right)^2 \frac{\partial^2}{\partial \chi_1 \partial \chi_2} \sum_{\epsilon_1 \epsilon_2} \text{Tr} (G \hat{V})^2, \quad (71) \end{aligned}$$

where $\hat{G} = \hat{A}_0^{-1}$ is the Green function of the diffusion operator: $[-\nabla^2 + |\varepsilon_1| + |\varepsilon_2|]G_{\varepsilon_1 \varepsilon_2}(x, y) = \delta(x - y)$, and Tr implies tracing over coordinates as well. Explicitly,

$$G_{\varepsilon_1 \varepsilon_2}(x, y) = \frac{\sinh \lambda(\frac{1}{2} + m) \sinh \lambda(\frac{1}{2} - M)}{\lambda \sinh \lambda}, \quad (72)$$

where $m = \min(x, y)$, $M = \max(x, y)$, and $\lambda = \sqrt{|\varepsilon_1| + |\varepsilon_2|}$.

We start with the *weak localization correction*. Expanding

$$\hat{V}(x) = V^0(x) + V^1(x)\hat{\Sigma}_1 + V^3(x)\hat{\Sigma}_3, \quad (73)$$

with $V^i(x)$ given by Eqs. (D4)–(D6), we get for the expression entering Eq. (70):

$$\text{Tr} G \hat{\Sigma}_3 V_{\epsilon, -\epsilon}^{\chi\chi} = 2 \int_{-1/2}^{1/2} dx G_{\epsilon, -\epsilon}(x, x) (V^3(x))_{\epsilon, -\epsilon}^{\chi\chi}. \quad (74)$$

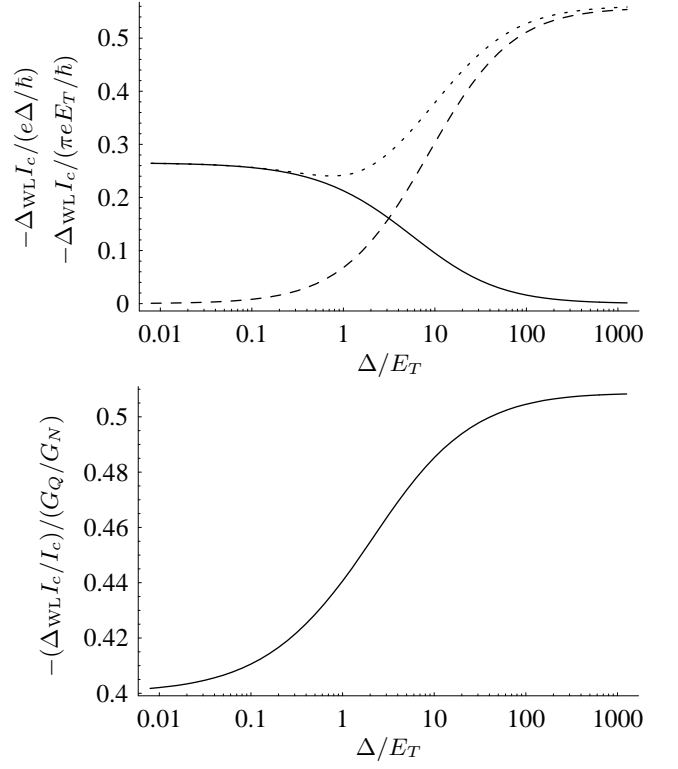


FIG. 11: (a) Weak localization correction to the critical current $-\Delta_{\text{WL}}I_c$ (solid line: in units of $e\Delta/\hbar$, dashed line: in units of $\pi eE_g/\hbar$, dotted line: in units of eE_*/\hbar) vs. Δ/E_T at zero temperature. (b) The ratio $-\Delta_{\text{WL}}I_c/I_c$ (in units of G_Q/G_N) vs. Δ/E_T at zero temperature.

Evaluating the integral using Eqs. (72) and (D6) we obtain the weak localization correction:

$$\Delta_{\text{WL}}I(\chi) = -\frac{ekT}{8\hbar} \sin \chi \sum_{\epsilon} \frac{\Delta^2 \cosh 2\kappa}{\epsilon^2 \sinh^3 \kappa} (2\kappa - \tanh 2\kappa), \quad (75)$$

where $\kappa = \sqrt{2|\varepsilon|} = \sqrt{2|\epsilon|/E_T}$.

For short junctions ($kT_c \ll E_T$),

$$\Delta_{\text{WL}}I(\chi) = -\frac{e\Delta^2}{12\hbar kT} \sin \chi, \quad (76)$$

and $\Delta_{\text{WL}}I(\chi)/I(\chi) = -G_Q/3G_N$.

For long junctions ($E_T \ll kT_c$),

$$\Delta_{\text{WL}}I(\chi) = -\frac{4}{\pi} \frac{e\Delta^2}{\hbar \sqrt{2\pi kT E_T}} e^{-\sqrt{2\pi kT/E_T}} \sin \chi, \quad (77)$$

and $\Delta_{\text{WL}}I(\chi)/I(\chi) = -G_Q/2G_N$.

Mesoscopic fluctuations are calculated in Appendix D with the help of Eq. (71). The result has the form

$$\begin{aligned} \langle\langle I(\chi_1)I(\chi_2) \rangle\rangle &= 4 \left(\frac{ekT}{\hbar} \right)^2 \sin \chi_1 \sin \chi_2 \\ &\times \sum_{\epsilon_1 \epsilon_2} \frac{\Delta^4}{\epsilon_1^2 \epsilon_2^2} \left(\frac{\kappa_1}{\sinh \kappa_1} \right)^2 \left(\frac{\kappa_2}{\sinh \kappa_2} \right)^2 \Upsilon_{\varepsilon_1 \varepsilon_2}, \quad (78) \end{aligned}$$

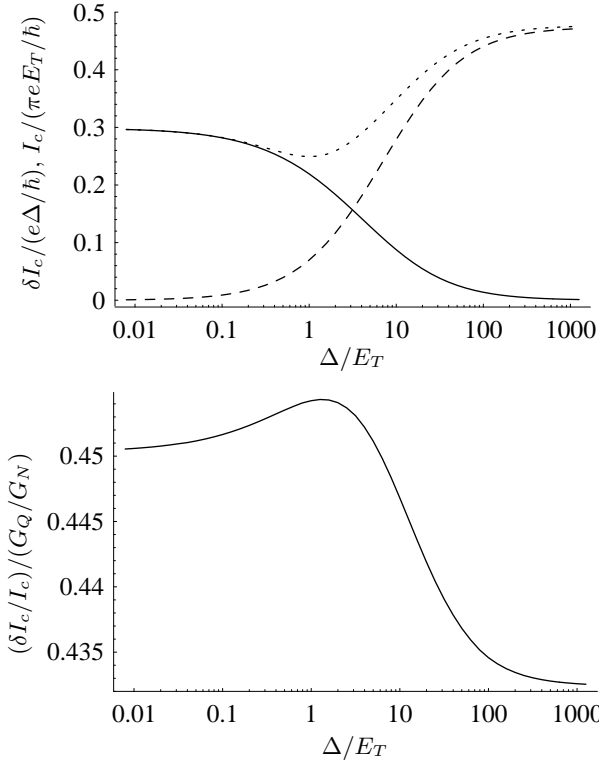


FIG. 12: (a) The amplitude of mesoscopic fluctuations of the critical current δI_c (solid line: in units of $e\Delta/\hbar$, dashed line: in units of $\pi e E_T/\hbar$, dotted line: in units of $e E_*/\hbar$) vs. Δ/E_T at zero temperature. (b) The ratio $\delta I_c/I_c$ (in units of G_Q/G_N) vs. Δ/E_T at zero temperature.

where the function $\Upsilon_{\varepsilon_1 \varepsilon_2}$ is defined in Eq. (D10).

For short junctions ($kT_c \ll E_T$), one can take the limit $\kappa_1, \kappa_2, \lambda \rightarrow 0$ and get $\Upsilon_{\varepsilon_1 \varepsilon_2} = 1/30$, leading to

$$\langle\langle I(\chi_1)I(\chi_2) \rangle\rangle = \frac{1}{120} \left(\frac{e\Delta^2}{\hbar kT} \right)^2 \sin \chi_1 \sin \chi_2. \quad (79)$$

This result could have been deduced already from the exact result (66) for short junctions. The relative fluctuations of the Josephson current are $\delta I(\chi)/I(\chi) = \sqrt{2/15} G_Q/G_N$.

For long junctions ($E_T \ll kT_c$), the sums in Eq. (78) are dominated by the lowest Matsubara frequencies $\varepsilon_1, \varepsilon_2 = \pm\pi T$, and $\Upsilon_{\pi T, \pi T} = e^{2\kappa}/128\kappa^2$ with $\kappa = \kappa_1 = \kappa_2$. Hence

$$\langle\langle I(\chi_1)I(\chi_2) \rangle\rangle = \frac{4e^2\Delta^4}{\pi^3\hbar^2 kT E_T} e^{-\sqrt{8\pi kT/E_T}} \sin \chi_1 \sin \chi_2, \quad (80)$$

and the relative mesoscopic fluctuations are $\delta I(\chi)/I(\chi) = G_Q/2\sqrt{2}G_N$.

3. Arbitrary wire at zero temperatures

Finally, we discuss the case of an arbitrary wire at zero temperature, when the problem can be solved only

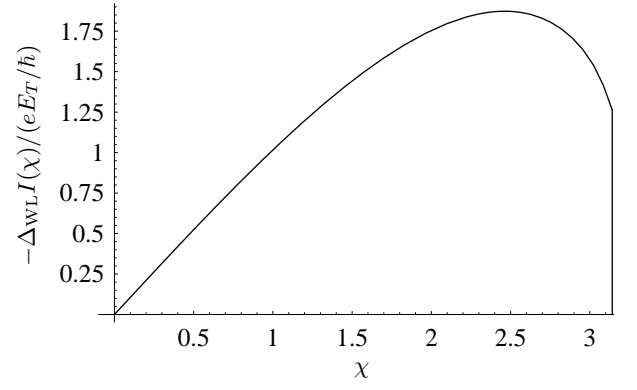


FIG. 13: Weak localization correction $-\Delta_{\text{WL}}I(\chi)$ (in units of eE_T/\hbar) vs. χ for long wires at zero temperature.

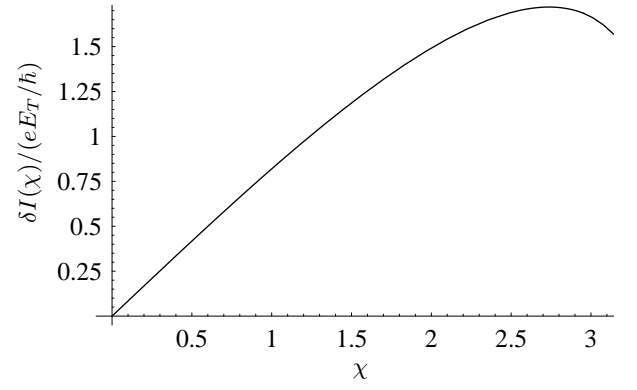


FIG. 14: Mesoscopic fluctuations $\delta I(\chi)$ (in units of eE_T/\hbar) vs. χ for long wires at zero temperature.

numerically. Here, the amplitude of mesoscopic fluctuations, $\delta I(\chi)$, and WL correction, $\Delta_{\text{WL}}I(\chi)$, are functions of two parameters: the ratio Δ/E_T and the phase difference χ .

The dependencies of the WL correction to the critical current and its mesoscopic fluctuations on Δ/E_T are presented in Figs. 11 and 12, respectively. One can clearly see the crossover from the short to long limits at $\Delta \sim 5E_T$. Note that the relative magnitude of mesoscopic fluctuations shown in Fig. 12(b) is nearly insensitive to the wire's length and can be approximated by $\delta I_c/I_c \sim 0.44G_Q/G_N$.

For long junctions ($E_T \ll \Delta$), the energy scale for mesoscopic fluctuations is set by the Thouless energy: $\delta I_c = 1.490eE_T/\hbar$ and $\Delta_{\text{WL}}I_c = -1.754eE_T/\hbar$. The χ -dependences of the WL correction and mesoscopic fluctuations in this regime are shown in Figs. 13 and 14, respectively. These plots are inaccurate in the vicinity of $\chi = \pi$, cf. discussion in Sec. III B 1.

Note that our result for the magnitude of mesoscopic fluctuations of the critical current for long wires is 2.5 times larger than the prediction of Ref. 5.

TABLE II: Summary of results for a wire with conductance G_N contacted to superconducting leads.

	$\chi_c/(\pi/2)$	eI_c/G_N	$\hbar\delta I_c/e$	$g_N\delta I_c/I_c$	$\hbar\Delta_{\text{WL}}I_c/e$	$g_N\Delta_{\text{WL}}I_c/I_c$
$\Delta \ll E_T, T = 0$	1.255	$2.082\Delta^{[11]}$	$0.30\Delta^{[16,17]}$	0.45	$-0.266\Delta^{[16]}$	-0.401
$E_T \ll \Delta, T = 0$	1.271	$10.83E_T^{[13]}$	$1.490E_T$	0.432	$-1.754E_T$	-0.509
arb. $E_T/\Delta, T = 0$	Fig.7(a)	Fig.7(b) ^[13]	Fig. 12(a)	Fig. 12(b)	Fig. 11(b)	Fig. 11(b)
$kT \lesssim kT_c \ll E_T$	1	$\pi\Delta^2(T)/4kT_c^{[11]}$	$\Delta^2(T)/\sqrt{120}kT$	$\sqrt{2/15}$	$-\Delta^2(T)/12kT$	-1/3
$E_T \ll kT \lesssim kT_c$	1	$8\Delta^2(T)/\mathcal{E}^{[12]}$	$2^{3/2}\Delta^2(T)/\pi\mathcal{E}$	$1/(2\sqrt{2})$	$-4\Delta^2(T)/\pi\mathcal{E}$	-1/2

Here, $g_N = G_N/G_Q$, $\Delta(T) = [(8\pi^2/7\zeta(3))k^2T_c(T_c - T)]^{1/2}$, and $\mathcal{E} = \sqrt{2\pi kTE_T} \exp(\sqrt{2\pi kT/E_T})$.

C. Summary of results

The results of this Section are summarized in Table II. The critical current at low temperatures is related to the minigap in the normal region at $\chi = 0$, $E_* \sim \min(E_T, \Delta)$, through an Ambegaokar-Baratoff like formula: $I_c \sim G_N E_*/e$. We see that, quite generally, mesoscopic fluctuations and WL correction to the Josephson current are suppressed by the factor G_Q/G_N : $\delta I_c \sim -\Delta_{\text{WL}}I_c \sim eE_*/\hbar$, where the precise coefficients in this expression depend on the wire's length and temperature. Note that contrary to the S-QD-S cases considered in Sec. II, these coefficient are always of the order of 1. This should be compared to the behavior of the conductance. In a normal metallic wire, conductance fluctuations and its weak localization correction are also suppressed by the same factor G_Q/G_N , but the coefficients are ‘‘universal’’: $\delta G_N = \sqrt{2/15}G_Q$ and $\Delta_{\text{WL}}G_N = -G_Q/3$.

Note that for short wires at T close to T_c , the relative WL correction and mesoscopic fluctuations of I_c coincide with those of the conductance. This is due to the relation $I(\chi) \propto G \sin \chi$, see discussion in the end of Sec. IIF.

IV. MESOSCOPIC FLUCTUATIONS IN 2D AND 3D GEOMETRIES

A. Mesoscopic fluctuations of the Josephson current through a 2D electron gas

In Ref. 23, mesoscopic fluctuations of the critical current had been measured in junctions formed by a two-dimensional electron gas whose width W was much longer than the distance L between the superconducting electrodes. In this case, the results of Sec. III cannot be applied since transverse diffusive modes become relevant. In this Section we take them into account and calculate rms δI_c for the two-dimensional geometry.

Mesoscopic fluctuations can be obtained with the help of the general formula (38), where now the operator \hat{A} reads

$$\hat{A}^{(2D)}(x, y) = -\frac{\partial^2}{\partial y^2} + \hat{A}(x). \quad (81)$$

Here, $\hat{A}(x)$ stands for the operator (62) for the quasi-1D wire, and $-1/2 < x < 1/2$ ($0 < y < W/L$) is the dimensionless coordinate along (perpendicular to) the junction.

The eigenvalues of the operator (81) are given by

$$\lambda_{m,i} = \frac{\pi^2 m^2}{\eta^2} + \lambda_i, \quad (82)$$

where $\eta = W/L$, and λ_i are the eigenvalues of the operator $\hat{A}(x)$ (we suppressed the indices χ_1, χ_2 and $\varepsilon, \varepsilon'$ for brevity). For wires, only the zeroth transverse diffusive mode with $m = 0$ was relevant, whereas for the film geometry one has to sum over all m 's. As a result, we can express the current cumulant in terms of the spectrum of the operator $\hat{A}(x)$:

$$\langle\langle I(\chi_1)I(\chi_2) \rangle\rangle = -8 \left(\frac{ekT}{\hbar} \right)^2 \frac{\partial^2}{\partial \chi_1 \partial \chi_2} \sum_{\varepsilon\varepsilon'} \text{tr} F(A_{\varepsilon\varepsilon'}^{\chi_1\chi_2}), \quad (83)$$

where

$$F(\lambda) = \ln \left(\frac{\sqrt{\lambda}}{\eta} \sinh \eta\sqrt{\lambda} \right) \quad (84)$$

is a generalization of the function $\ln \lambda$ relevant for wires to arbitrary ratios $\eta = W/L$.

We analyze Eqs. (83) and (84) in the experimentally relevant limit²³ of wide ($W \gg L$) and long ($E_T \equiv \hbar D/L^2 \ll \Delta$) junctions, at small temperatures ($kT \ll E_T$). Then $F(\lambda) \approx \eta\sqrt{\lambda}$, and the spectral sum should be calculated numerically, analogously to the quasi-one-dimensional situation, see Sec. III B 3. We obtain for the rms of the critical current fluctuations (at $\chi_c = 1.27\pi/2$):

$$\delta I_c = 1.5 \frac{eE_T}{\hbar} \sqrt{\frac{W}{L}}. \quad (85)$$

A similar equation with the prefactor 2.2 was used in Ref. 23 [see Eq. (2) there] as the theoretical estimate for the critical current fluctuations. Though the two-dimensional case was not considered by Altshuler and Spivak⁵, it was claimed that Eq. (2) of Ref. 23 can be obtained from the three-dimensional result of Ref. 5. We could not follow the derivation of Eq. (2) in Ref. 23 but would like to emphasize that even the three-dimensional result for δI_c from Ref. 5 is overestimated in Eq. (1) of

Ref. 23 by the factor of π^2 due a different definition of the Thouless energy. So we expect that the 2D result for δI_c obtained within the Altshuler-Spivak approach would have the form (85) with the prefactor smaller than 1.

Thus, even though the approach of Ref. 5 generally underestimates the magnitude of critical current fluctuations, the theoretical prediction of Ref. 23 overestimated them by the factor of 1.5.

With the help of Eq. (85) we have a better explanation of experimental results (in the weakly localized regime I) from Ref. 23: $\delta I_c^{\text{theor}} = 45$ nA, $\delta I_c^{\text{exper}} = 15$ nA. Still, discrepancy by the factor of 3 remains.

For completeness, we present also the result for wide ($W \gg L$) and short ($\Delta \ll E_T$) junctions at $T = 0$. It can be obtained using the spectrum found in Sec. III B 1. We get for the rms of the critical current fluctuations:

$$\delta I_c = 0.26 \frac{e\Delta}{\hbar} \sqrt{\frac{W}{L}}. \quad (86)$$

B. 3D case

Finally, we mention that the above results for the 2D case can be easily generalized to the 3D case. To be specific, we consider the limit of wide junctions, when both transverse dimensions are large: $W_y, W_z \gg L$. Then, mesoscopic fluctuations can be found with the help of Eq. (83) with $F(\lambda) = (W_y W_z / 4\pi L^2) \lambda \ln M/\lambda$, where $M \sim L/l$ is the high-momentum cutoff [it drops from the answer since $\partial^2 \text{tr} \hat{A} / \partial \chi \partial \chi' = 0$, see Eq. (62)].

For long junctions ($E_T \ll \Delta$) at $T = 0$, numerical integration leads to Eq. (2). Note that the result of Ref. 5 obtained in the same limit contains the numerical factor $\sqrt{15\zeta(5)/\pi^3} = 0.71$ instead of 2.0. Again, we see that the approach of Ref. 5 underestimates the magnitude of mesoscopic fluctuations of I_c by a factor of 2.8.

For short junctions ($\Delta \ll E_T$) at $T = 0$, we obtain

$$\delta I_c = 0.28 \frac{e\Delta}{\hbar} \sqrt{\frac{W_y W_z}{L^2}}. \quad (87)$$

V. CONCLUSION

In this work, we used the replica σ -model technique to describe mesoscopic fluctuations and weak localization correction to the equilibrium supercurrent in Josephson junctions formed of a metallic wire between superconducting leads. We considered two types of junctions: a chaotic dot coupled to superconductors by tunnel barriers (S-QD-S) and a diffusive wire (SNS) with transparent NS interfaces. In both cases we calculated the amplitude of supercurrent fluctuations and the weak localization correction to the average current $I(\chi)$ in different temperature regions at arbitrary ratios between Δ and E_{dwell} (given by E_g for an S-QD-S junction, and by E_T for an SNS junction).

For a quasi-one-dimensional SNS junction, we have found that mesoscopic corrections to the quasiclassical Josephson current are “nearly universal”: $\delta I_c/I_c \sim -\Delta_{\text{WL}} I_c/I_c \sim G_Q/G$, where the exact coefficients in these relations are of the order of 1, being slightly dependent on the parameters of the junction. For a double-barrier S-QD-S junction, the weak localization correction vanishes, while mesoscopic fluctuations are “less universal”: $\delta I_c/I_c \sim G_Q/G$ for junctions with $kT_c \ll E_g$, and is additionally suppressed for junctions with $E_g \ll kT_c$.

We also demonstrate that the approach of Ref. 5 systematically underestimates the magnitude of mesoscopic fluctuations of the critical current by factors around 2.5–2.8, both in the quasi-one-dimensional and three-dimensional cases.

Theoretical predictions for the mesoscopic fluctuations of the critical current should be compared with experimental results.^{23,24} In Ref. 23, mesoscopic fluctuations of I_c were studied in a geometry of wide ($W \gg L$) long ($E_T \ll \Delta$) bar of a two-dimensional electron gas. Experimentally observed fluctuation magnitude (in the weakly localized regime I) is three times smaller than our result (85). Experiment of Ref. 24 refers to the quasi-one-dimensional short ($\Delta \ll E_T$) wires, and should be compared with the result^{16,17} $\delta I_c = 0.30e\Delta/\hbar$. Again, theoretical prediction (~ 7 nA) appears to be several times larger than the experimentally measured magnitude. This systematic discrepancy might be attributed either to the effect of electron-electron interaction or to non-ideal transparencies of the NS interfaces.

Among the motivations to study mesoscopic fluctuations, it was suggested that they may induce the sign change of the critical current (π -junction behavior).⁴² However, such possibility was discarded in Ref. 43 if time-reversal symmetry is preserved in the normal part, and if interactions are absent. If the normal part is ferromagnetic, time-reversal symmetry is broken. Then, with strong barriers between the wire and leads, it was shown that mesoscopic fluctuations are dominant in the Josephson relation compared to the quasiclassical contribution.⁴⁴ Within our approach this study could be easily reconsidered and extended by adding an exchange energy term in the Hamiltonian of the wire. A strong Coulomb blockade in the central dot was also shown to provide a mechanism of π -junction formation via fluctuations.⁴⁵ We note that the replica σ -model is also appropriate for taking electron-electron interactions into account. This could be the subject of future study.

Acknowledgments

We thank M. V. Feigelman, Ya. V. Fominov, and L. I. Glazman for useful discussions. The work of M.A.S. was supported by the RFBR under grant No. 04-02-16998, and the Russian Science Support Foundation.

APPENDIX A: SOLUTION OF THE USADEL EQUATIONS FOR A WIRE

1. Determination of the spectral current J and $\theta(0)$

For a fixed $\varepsilon > 0$, θ_s and χ , the values of the spectral current J and the Usadel angle $\theta_0 \equiv \theta(0)$ in the middle of the wire are determined from two equations:

$$\sqrt{\varepsilon} = \int_{\theta_0}^{\theta_s} \frac{d\theta}{\mathcal{R}(\theta)}, \quad (\text{A1a})$$

$$\chi = 2\sqrt{\alpha} \int_{\theta_0}^{\theta_s} \frac{1}{\sin^2 \theta \mathcal{R}(\theta)} d\theta, \quad (\text{A1b})$$

where $\mathcal{R}(\theta) = [\cos \theta_0 - \cos \theta + \alpha(\sin^{-2} \theta_0 - \sin^{-2} \theta)]^{1/2}$ and $\alpha = J^2/4\varepsilon$. These integrals can be converted to the standard elliptic integrals:

$$\sqrt{\varepsilon} = \frac{2F(\varphi, k)}{\sqrt{a-c}}, \quad (\text{A2a})$$

$$\chi = \frac{4\sqrt{\alpha}F(\varphi, k)}{(1-a^2)\sqrt{a-c}} + \frac{2\sqrt{\alpha}(b-a)}{\sqrt{a-c}} \times \left[\frac{\Pi(\varphi, k^2 \frac{1-a}{1-b}, k)}{(1-a)(1-b)} - \frac{\Pi(\varphi, k^2 \frac{1+a}{1+b}, k)}{(1+a)(1+b)} \right], \quad (\text{A2b})$$

where

$$\begin{cases} a \\ c \end{cases} = \frac{\alpha}{2\sin^2 \theta_0} \pm \sqrt{1 + \frac{\alpha \cos \theta_0}{\sin^2 \theta_0} + \frac{\alpha^2}{4\sin^4 \theta_0}}, \quad (\text{A3a})$$

$$b = \cos \theta_0, \quad k = \sqrt{\frac{b-c}{a-c}}, \quad (\text{A3b})$$

$$\varphi = \arcsin \sqrt{\frac{(a-c)(b-\cos \theta_s)}{(b-c)(a-\cos \theta_s)}}. \quad (\text{A3c})$$

Note that our definition of elliptic integrals $F(\varphi, k)$ and $\Pi(\varphi, n, k)$ coincides with that of Ref. 34. The same functions are often defined in a different way⁴⁶: in Mathematica, e.g., $F(\varphi, k) = \text{EllipticF}[\varphi, k^2]$, and $\Pi(\varphi, n, k) = \text{EllipticPi}[n, \varphi, k^2]$.

Equations (A2) should be solved numerically to obtain α and b (and hence J and θ_0) for given $\varepsilon > 0$, θ_s and χ . The Usadel angles for $\varepsilon < 0$ can be obtained from Eqs. (49).

2. Determination of $\theta(x)$ and $\eta(x)$

For each ε we first have to find θ_0 and α as described above. Then for a spacial point x_i , the value $\theta_i = \theta(x_i)$ can be found from the equation

$$|x_i| = \frac{F(\varphi_i, k)}{\sqrt{\varepsilon}\sqrt{a-c}}, \quad \varphi_i = \arcsin \sqrt{\frac{(a-c)(b-\cos \theta_i)}{(b-c)(a-\cos \theta_i)}}, \quad (\text{A4})$$

which can be solved as

$$\cos \theta_i = \frac{b-aY}{1-Y}, \quad Y = \frac{b-c}{a-c} \text{sn}^2(|x_i|\sqrt{\varepsilon(a-c)}, k), \quad (\text{A5})$$

where $\text{sn}(u, k)$ is the Jacobi elliptic function³⁴. In Mathematica, e.g., $\text{sn}(u, k) = \text{JacobiSN}[u, k^2]$.

Then we determine $\eta_i = \eta(x_i)$ from Eq. (65):

$$\eta_i = -\frac{\sqrt{\alpha}}{2} \int_{\theta_0}^{\theta_i} \frac{1}{(\cos \theta_0 - \cos \theta) + \frac{\alpha}{\sin^2 \theta_0} \mathcal{R}(\theta)} d\theta. \quad (\text{A6})$$

Converting this to elliptic integrals and using Eq. (A4) we get

$$\eta_i = -\frac{\sqrt{\varepsilon\alpha} x_i}{(p-a)} - \frac{x_i}{|x_i|} \frac{\sqrt{\alpha}(b-a)}{\sqrt{a-c}} \frac{\Pi(\varphi_i, k^2 \frac{p-a}{p-b}, k)}{(p-a)(p-b)}, \quad (\text{A7})$$

where $p = \cos \theta_0 + \alpha/\sin^2 \theta_0$. Note that $\eta(x)$ is an odd function of x .

The functional determinants of $\hat{A}(x)$ involved in Eqs. (33) and (38) can be calculated numerically by introducing a proper grid x_i . Then we discretize the Laplace operator in the operator \hat{A} [Eq. (62)], and find α_{mn} , ρ_{mn} , η_m and η_n for each x_i , thus defining a finite matrix \hat{A}_{ij} . The functional determinants in Eqs. (33) and (38) can then be approximated by determinants of the matrix \hat{A}_{ij} which should be evaluated numerically.

APPENDIX B: DERIVATION OF THE OPERATOR A FOR A WIRE

Substituting Eq. (21) into (46) and expanding the action to the second order in W , we get:

$$S^{(2)} = \frac{G_N}{16G_Q} \int_{-1/2}^{1/2} dx \text{tr} \left[-(\nabla W)^2 + \{\mathcal{J}, W\}^2 - 2\mathcal{J}\tau_1[W, \nabla W] - 2\varepsilon U\tau_3 U^\dagger \tau_1 W^2 \right], \quad (\text{B1})$$

where $\mathcal{J} = U\nabla U^\dagger \tau_1$. Using the decomposition (25) of W in terms of the d - and c -modes, we rewrite $S^{(2)}$ in the form (61), where

$$\hat{A}_{mn}(x) = -\nabla^2 + \alpha_{mn} + \lambda_{mn}^2/4 - i\hat{\Sigma}_2[\lambda_{mn}\nabla + (\nabla\lambda_{mn})/2] + \beta_{mn}\hat{\Sigma}_3 + \gamma_{mn}\hat{\Sigma}_1. \quad (\text{B2})$$

Here, $m = (\varepsilon, a)$ and $n = (\varepsilon', b)$ are energy and replica indices, $\hat{\Sigma}_{i=1,2,3}$ are the Pauli matrices in the (d, c) -space, α_{mn} is given by Eq. (63), and

$$\lambda_{mn} = -(\cos \theta_n \nabla \phi_n + \cos \theta_m \nabla \phi_m), \quad (\text{B3a})$$

$$\beta_{mn} = (\sin \theta_n \nabla \phi_n \sin \theta_m \nabla \phi_m - \nabla \theta_n \nabla \theta_m)/2, \quad (\text{B3b})$$

$$\gamma_{mn} = -(\sin \theta_n \nabla \phi_n \nabla \theta_m + \sin \theta_m \nabla \phi_m \nabla \theta_n)/2. \quad (\text{B3c})$$

Here, (θ_m, ϕ_m) and (θ_n, ϕ_n) are the solutions of the Usadel equations (48) at energies ε and ε' , and phase difference χ_1 or χ_2 , depending on the replica indices a and b , respectively.

In order to remove the first order derivative in Eq. (B2), we make a local unitary transformation in the (d, c) -space: $(d, c)_{mn}^T \rightarrow \mathcal{V}_{mn}(d, c)_{mn}^T$, where

$$\mathcal{V}_{mn} = \cos \frac{\zeta_n + \zeta_m}{2} - i \hat{\Sigma}_2 \sin \frac{\zeta_n + \zeta_m}{2}, \quad (\text{B4a})$$

$$\zeta_m(x) = - \int_0^x ds \cos \theta_m(s) \nabla \phi_m(s). \quad (\text{B4b})$$

Such a rotation leaves $\det \hat{A}$ and $A_{\varepsilon, -\varepsilon}^{\chi\chi}$ invariant, while the operator \hat{A} is transformed to

$$\hat{A} = \mathcal{V}_{mn}^\dagger \hat{A}_{mn} \mathcal{V}_{mn}, \quad (\text{B5})$$

that can be written in the form (62) (tilde omitted) with

$$\eta_m = - \arctan \frac{\nabla \theta_m}{\sin \theta_m \nabla \phi_m} - \zeta_m. \quad (\text{B6})$$

Taking the derivative of (B6), we come to Eq. (65).

APPENDIX C: EQUIVALENCE OF EQ. (66) TO THE RESULTS OF REFS. 16 AND 17

The result for the variance of the Josephson current, $\text{var } I(\chi) = \delta I^2(\chi)$, obtained in Refs. 16 and 17 can be written in the form

$$\text{var } I(\chi) = \frac{1}{2} \left(\frac{e\Delta}{\pi\hbar} \right)^2 \int_0^\infty dk k (1 - e^{-\pi k}) |a(k)|^2, \quad (\text{C1})$$

$$a(k) = \int_0^\infty \frac{dx \cos kx \sin \chi}{\cosh x \sqrt{\cosh^2 x - \sin^2 \frac{\chi}{2}}}. \quad (\text{C2})$$

In this Appendix we show that our expression (66) for $\langle\langle I(\chi)I(\chi') \rangle\rangle$ at $\chi' = \chi$ and zero temperature gives the same result.

We start with rewriting Eq. (66) in the form of integrals over C and C' :

$$\text{var } I(\chi) = -\frac{1}{2} \left(\frac{e\Delta}{\pi\hbar} \right)^2 \int_0^{\chi/2} \frac{dC \sin \chi}{\sin C \sqrt{\sin^2 \frac{\chi}{2} - \sin^2 C}} \frac{dC' \sin \chi}{\sin C' \sqrt{\sin^2 \frac{\chi}{2} - \sin^2 C'}} \frac{\partial^2}{\partial C \partial C'} \ln \frac{\sin(C - C') \sin(C + C')}{C - C' C + C'}. \quad (\text{C3})$$

Using Eqs. (2.29) and (3.6) from Ref. 16, we rewrite the second derivative of the logarithm as

$$\frac{\partial^2}{\partial C \partial C'} \ln \frac{\sin(C - C') \sin(C + C')}{C - C' C + C'} = -4 \int_0^\infty dk \frac{k \sinh kC \sinh kC'}{e^{\pi k} - 1}, \quad (\text{C4})$$

which allows to present Eq. (C3) in the form (C1) with $\tilde{a}(k)$ instead of $a(k)$:

$$\tilde{a}(k) = \frac{1}{\sinh(\pi k/2)} \int_0^{\chi/2} \frac{dC \sinh kC \sin \chi}{\sin C \sqrt{\sin^2 \frac{\chi}{2} - \sin^2 C}}. \quad (\text{C5})$$

The equivalence between our result and the result of Refs. 16 and 17 follows from the equality $a(k) = \tilde{a}(k)$. To prove it, we extend integration in Eq. (C2) to the real axis, substituting $\cos kx$ by e^{ikx} . Then we deform the integration contour to the upper half-plane and enclose all branch cuts of the square root: $[i(\pi n + \pi/2 - \chi/2), i(\pi n + \pi/2 + \chi/2)]$, $n = 0, 1, \dots$. As a result, summation of $e^{-(n+1/2)\pi k}$ over n yields $\sinh(\pi k/2)$ in the denominator, while integration along the branch cut reproduces the integral in Eq. (C5). Thus, $a(k) = \tilde{a}(k)$ which establishes the equivalence between the two results.

APPENDIX D: SOLUTION OF THE USADEL EQUATION FOR A WIRE CLOSE TO T_c

Close to T_c , the solution of the Usadel equation (48) is given by Eq. (57). It corresponds to the following dependence of $\theta(x)$ and $\phi(x)$:

$$\sin \theta(x) = \frac{\sin \theta_s}{\sinh \kappa} \sqrt{\cosh 2\kappa x (\cosh \kappa - \cos \chi) - (1 - \cosh \kappa \cos \chi)}, \quad (\text{D1})$$

$$\tan \phi(x) = \frac{\tan \frac{\chi}{2}}{\tanh \frac{\kappa}{2}} \tanh \kappa x \quad (\text{D2})$$

(this form is valid both for $\varepsilon > 0$ and $\varepsilon < 0$). The function $\eta(x)$ defined in Eq. (65) is given by

$$\tan \eta(x) = - \text{sign}(\varepsilon) \frac{\tanh \frac{\kappa}{2}}{\tan \frac{\chi}{2}} \tanh \kappa x. \quad (\text{D3})$$

Rigidity of Gaussian fluctuations near the saddle point is determined by the operator $\hat{A}_{\varepsilon_1\varepsilon_2} = -\nabla^2 + |\varepsilon_1| + |\varepsilon_2| + \hat{V}_{\varepsilon_1\varepsilon_2}$, where the operator \hat{V} can be expanded in the Pauli matrices (73) with the coefficients

$$V^0(x) = -\frac{1}{2} \left(\frac{\Delta}{|\varepsilon_1|} \frac{\kappa_1}{\sinh \kappa_1} \right)^2 (\cosh \kappa_1 - \cos \chi_1) \cosh 2\kappa_1 x - \frac{1}{2} \left(\frac{\Delta}{|\varepsilon_2|} \frac{\kappa_2}{\sinh \kappa_2} \right)^2 (\cosh \kappa_2 - \cos \chi_2) \cosh 2\kappa_2 x, \quad (D4)$$

$$V^1(x) = -2 \frac{\Delta}{|\varepsilon_1|} \frac{\kappa_1}{\sinh \kappa_1} \frac{\Delta}{|\varepsilon_2|} \frac{\kappa_2}{\sinh \kappa_2} \left(\text{sign}(\varepsilon_1) \cos \frac{\chi_1}{2} \sin \frac{\chi_2}{2} \sinh \frac{\kappa_1}{2} \cosh \frac{\kappa_2}{2} \sinh \kappa_1 x \cosh \kappa_2 x \right. \\ \left. + \text{sign}(\varepsilon_2) \sin \frac{\chi_1}{2} \cos \frac{\chi_2}{2} \cosh \frac{\kappa_1}{2} \sinh \frac{\kappa_2}{2} \cosh \kappa_1 x \sinh \kappa_2 x \right), \quad (D5)$$

$$V^3(x) = 2 \frac{\Delta}{|\varepsilon_1|} \frac{\kappa_1}{\sinh \kappa_1} \frac{\Delta}{|\varepsilon_2|} \frac{\kappa_2}{\sinh \kappa_2} \left(\sin \frac{\chi_1}{2} \sin \frac{\chi_2}{2} \cosh \frac{\kappa_1}{2} \cosh \frac{\kappa_2}{2} \cosh \kappa_1 x \cosh \kappa_2 x \right. \\ \left. - \text{sign}(\varepsilon_1\varepsilon_2) \cos \frac{\chi_1}{2} \cos \frac{\chi_2}{2} \sinh \frac{\kappa_1}{2} \sinh \frac{\kappa_2}{2} \sinh \kappa_1 x \sinh \kappa_2 x \right). \quad (D6)$$

The supercurrent correlation function (71) involves

$$R_{\varepsilon_1\varepsilon_2} = \text{Tr}(G\hat{V})^2 = 2 \int_{-1/2}^{1/2} dx dy G_{\varepsilon_1\varepsilon_2}^2(x, y) \sum_{i=0,1,3} V^i(x)V^i(y). \quad (D7)$$

Since current fluctuations are determined by $\sum_{\varepsilon_1, \varepsilon_2} R_{\varepsilon_1\varepsilon_2}$, it is convenient to symmetrize R by introducing

$$\tilde{R}_{\varepsilon_1, \varepsilon_2} = \frac{1}{4} [R_{\varepsilon_1, \varepsilon_2} + R_{-\varepsilon_1, \varepsilon_2} + R_{\varepsilon_1, -\varepsilon_2} + R_{-\varepsilon_1, -\varepsilon_2}], \quad (D8)$$

such that $\sum_{\varepsilon_1, \varepsilon_2} R_{\varepsilon_1\varepsilon_2} = \sum_{\varepsilon_1, \varepsilon_2} \tilde{R}_{\varepsilon_1\varepsilon_2}$.

Substituting Eqs. (D4)–(D6) into Eq. (D7), and taking the derivatives with respect to χ_1 and χ_2 we get

$$\frac{\partial^2}{\partial \chi_1 \partial \chi_2} \tilde{R}_{\varepsilon_1\varepsilon_2} = \left(\frac{\Delta}{|\varepsilon_1|} \frac{\kappa_1}{\sinh \kappa_1} \right)^2 \left(\frac{\Delta}{|\varepsilon_2|} \frac{\kappa_2}{\sinh \kappa_2} \right)^2 \Upsilon_{\varepsilon_1\varepsilon_2} \sin \chi_1 \sin \chi_2, \quad (D9)$$

resulting in Eq. (78). Here the function $\Upsilon_{\varepsilon_1\varepsilon_2}$ is defined by the double integral:

$$\Upsilon_{\varepsilon_1\varepsilon_2} = \int_{-1/2}^{1/2} dx dy G_{\varepsilon_1\varepsilon_2}(x, y)^2 \left[\cosh 2\kappa_1 x \cosh 2\kappa_2 y \right. \\ \left. + 2 \cosh^2 \frac{\kappa_1}{2} \cosh^2 \frac{\kappa_2}{2} \cosh \kappa_1 x \cosh \kappa_2 x \cosh \kappa_1 y \cosh \kappa_2 y + 2 \sinh^2 \frac{\kappa_1}{2} \sinh^2 \frac{\kappa_2}{2} \sinh \kappa_1 x \sinh \kappa_2 x \sinh \kappa_1 y \sinh \kappa_2 y \right. \\ \left. - 2 \cosh^2 \frac{\kappa_1}{2} \sinh^2 \frac{\kappa_2}{2} \cosh \kappa_1 x \sinh \kappa_2 x \cosh \kappa_1 y \sinh \kappa_2 y - 2 \sinh^2 \frac{\kappa_1}{2} \cosh^2 \frac{\kappa_2}{2} \sinh \kappa_1 x \cosh \kappa_2 x \sinh \kappa_1 y \cosh \kappa_2 y \right]. \quad (D10)$$

In principle, these integrals can be calculated in a closed form. However, the resulting expression is too complicated and we leave the integrals unevaluated.

¹ E. Abrahams, P. W. Anderson, D. C. Licciardello, and T. V. Ramakrishnan, Phys. Rev. Lett. **42**, 673 (1979); L. P. Gor'kov, A. I. Larkin, and D. E. Khmel'nitskii, Pis'ma Zh. Eksp. Theor. Fiz. **30**, 248 (1979) [JETP Lett. **30**, 228 (1979)].

² B. L. Altshuler, Pisma Zh. Eksp. Theor. Fiz. **51**, 530 (1985) [JETP Lett. **41**, 648 (1985)]; P. A. Lee and A. D. Stone, Phys. Rev. Lett **55**, 1622 (1985).

³ S. Washburn and R. A. Webb, Adv. Phys. **35**, 375 (1986).

⁴ *Mesoscopic Phenomena in Solids*, Eds. B. L. Altshuler, P. A. Lee, and R. A. Webb, Modern Problems in Condensed Matter Sciences vol. 30, North-Holland, 1991.

⁵ B. L. Altshuler and B. Z. Spivak, Zh. Eksp. Theor. Fiz. **92**, 607 (1987) [Sov. Phys. JETP **65**, 343 (1987)].

⁶ A. F. Andreev, Zh. Eksp. Theor. Fiz. **46**, 1823 (1964) [Sov. Phys. JETP **19**, 1228 (1964)].

- ⁷ B. Z. Spivak and D. E. Khmel'nitskii, Pis'ma Zh. Eksp. Theor. Fiz. **35**, 334 (1982) [JETP Lett. **35**, 412 (1982)].
- ⁸ W. L. McMillan, Phys. Rev. **175**, 537 (1968); A. A. Golubov and M. Yu. Kupriyanov, Zh. Eksp. Theor. Fiz. **96**, 1420 (1989) [Sov. Phys. JETP **69**, 805 (1989)]. J. A. Melsen, P. W. Brouwer, K. M. Frahm, and C. W. J. Beenakker, Europhys. Lett. **35**, 7 (1996), Phys. Scrip. **69**, 223 (1997).
- ⁹ K. D. Usadel, Phys. Rev. Lett. **25**, 507 (1970).
- ¹⁰ For this reason, the theory of Ref. 5 does not allow determining correctly the average Josephson current.
- ¹¹ I. O. Kulik and A. M. Omelyanchuk, Pisma Zh. Eksp. Theor. Fiz. **21**, 216 (1975) [JETP Lett. **21**, 96 (1975)].
- ¹² A. D. Zaikin and G. F. Zharkov, Fiz. Nizk. Temp. **7**, 375 (1981) [Sov. J. Low Temp. Phys. **7**, 184 (1981)].
- ¹³ P. Dubos, H. Courtois, B. Pannetier, F. K. Wilhelm, A. D. Zaikin, and G. Schön, Phys. Rev. B **63**, 064502 (2001).
- ¹⁴ A. A. Golubov, M. Yu. Kupriyanov, and E. Il'ichev, Rev. Mod. Phys. **76**, 411 (2004).
- ¹⁵ C. W. J. Beenakker, Rev. Mod. Phys. **69**, 731 (1997).
- ¹⁶ A. M. S. Macêdo and J. T. Chalker, Phys. Rev. B **49**, 4695 (1994).
- ¹⁷ C. W. J. Beenakker and B. Rejaei, Phys. Rev. B **49**, 7499 (1994).
- ¹⁸ C. W. J. Beenakker, Phys. Rev. Lett. **67**, 3836 (1991); Phys. Rev. Lett. **68**, 1442 (1992) (Erratum).
- ¹⁹ Y. Takane, J. Phys. Soc. Japan **63**, 2668 (1994); A. Furusaki, Physica B **203**, 214 (1994).
- ²⁰ T. Micklitz, e-print cond-mat/0701174.
- ²¹ K. B. Efetov, *Supersymmetry in Disorder and Chaos* (Cambridge University Press, New York, 1997).
- ²² A. Altland, B. D. Simons and D. Taras-Semchuk, Pisma Zh. Eksp. Theor. Fiz. **67**, 21 (1998) [JETP Lett. **67**, 22 (1998)]; Adv. Phys. **49**, 321 (2000).
- ²³ H. Takayanagi, J. B. Hansen, and J. Nitta, Phys. Rev. Lett. **74**, 166 (1995).
- ²⁴ Y.-J. Doh, J. A. van Dam, A. L. Roest, E. P. A. M. Bakkers, L. P. Kouwenhoven, and S. De Franceschi, Science **309**, 272 (2005).
- ²⁵ L. G. Aslamazov, A. I. Larkin, and Yu. N. Ovchinnikov, Zh. Eksp. Theor. Fiz. **55**, 323 (1968) [Sov. Phys. JETP **28**, 171 (1969)].
- ²⁶ M. Yu. Kupriyanov and V. F. Lukichev, Zh. Eksp. Theor. Fiz. **94** (6), 139 (1988) [Sov. Phys. JETP **67**, 1163 (1988)].
- ²⁷ P. W. Brouwer and C. W. J. Beenakker, Chaos, Solitons & Fractals **8**, 1249 (1997).
- ²⁸ S. F. Edwards and P. W. Anderson, J. Phys. F **5**, 965 (1975).
- ²⁹ F. J. Wegner, Z. Phys. B **35**, 207 (1979).
- ³⁰ K. B. Efetov, A. I. Larkin, and D. E. Khmel'nitskii, Zh. Eksp. Theor. Fiz. **79**, **1120**, (1980) [Sov. Phys. JETP **52**, **568** (1980)].
- ³¹ A. M. Finkel'stein, *Electron Liquid in Disordered Conductors*, volume 14 of *Soviet Scientific Reviews*, edited by I. M. Khalatnikov (Harwood Academic, London, 1990).
- ³² Y. Oreg, P. W. Brouwer, B. D. Simons, and A. Altland, Phys. Rev. Lett. **82**, 1269 (1999).
- ³³ Yu. V. Nazarov, Phys. Rev. Lett. **73**, 1420 (1994).
- ³⁴ I. S. Gradshteyn, I. M. Ryzhik, *Table of Integrals, Series, and Products* (Academic Press, 2000).
- ³⁵ P. M. Ostrovsky, M. V. Feigel'man, Pis'ma Zh. Eksp. Theor. Fiz. **82**, 863 (2005) [JETP Lett. **82**, 763 (2005)].
- ³⁶ S. Iida, H. A. Weidenmüller, and J. A. Zuk, Ann. Phys. (N.Y.) **200**, 219 (1990).
- ³⁷ C. W. J. Beenakker, Phys. Rev. B **47**, 15763 (1993).
- ³⁸ M. Houzet and L. I. Glazman, unpublished.
- ³⁹ F. Zhou, P. Charlat, B. Spivak, and B. Pannetier, J. Low Temp. Phys. **110**, 841 (1998).
- ⁴⁰ P. M. Ostrovsky, M. A. Skvortsov, and M. V. Feigel'man, Phys. Rev. Lett. **87**, 027002 (2001).
- ⁴¹ We use the same notation for the initial matrix \hat{A} and the rotated matrix $\mathcal{V}^\dagger \hat{A} \mathcal{V}$ since they give identical WL corrections and mesoscopic fluctuations.
- ⁴² B. I. Spivak and S. A. Kivelson, Phys. Rev. B **43**, 3740 (1991).
- ⁴³ M. Titov, Ph. Jacquod, and C. W. J. Beenakker, Phys. Rev. B **65**, 012504 (2002).
- ⁴⁴ A. Yu. Zyuzin, B. Spivak, and M. Hruska, Europhys. Lett. **62**, 97 (2003).
- ⁴⁵ A. V. Rozhkov, D. P. Arovos, and F. Guinea, Phys. Rev. B **64**, 233301 (2001).
- ⁴⁶ M. Abramowitz and I. A. Stegun, *Handbook of Mathematical Functions with Formulas, Graphs, and Mathematical Tables* (Dover, New York, 1964).